SPRAY FORMING AND TRIBOLOGICAL BEHAVIOUR OF SiC PARTICLE REINFORCED Al-Si ALLOY

Thesis submitted in partial fulfilment of the requirement for

The award of the degree of

Master of Technology (M. Tech)

In

MATERIALS AND METALLURGICAL ENGINEERING

Submitted by

RAMKISHOR

Roll No. : 600802018

Under the guidance of

Dr. O.P PANDEY

Head of the Department

School of Physics & Materials Science

School of Physics & Materials Science

Thapar University, Patiala

July 2010

CERTIFICATE

I hereby certify that the work which is being presented in the thesis entitled, ***Spray Forming and Tribological Behaviour of SiC Particle Reinforced Al-Si Alloy"*** *submitted by Mr. RAMKISHOR, Roll No. 600802018 in partial fulfillment of the requirements for the award of* ***MASTER OF TECHNOLOGY*** *in* ***"Materials and Metallurgical Engineering"*** *from the* ***School of Physics and Material Science*** *of* ***Thapar University, Patiala****, is an authentic record of my own work carried out under the supervision of Dr. O.P. Pandey refers other researcher's work, which are duty listed in the reference section.*

This is to certify that the above statement made by the candidate is correct and true to the best of my knowledge.

(Prof. O.P. Pandey)

Supervisor

Thapar University, Patiala-147001

Countersigned by:

Dr. O.P. Pandey,
Professor and Head of the Department,
Thapar University,
Patiala, Punjab.

Dr. R.K. Sharma
Dean Academic Affairs,
Thapar University,
Patiala, Punjab.

ACKNOWLEDGEMENT

The real sprit of achieving a goal is through the way of excellence and austere discipline. I would have never succeeded in completing my task without the cooperation, encouragement and help provided to me by various personalities.

With deep sense of gratitude I express thanks to my esteemed and worthy supervisor ***Dr.O.P.Pandey*** *, Professor & Head of SI'MS, for his valuable guidance in carrying out this work under his effective supervision, encouragement and cooperation.*

I shall be failing in duties if I do not express my deep sense of gratitude toward ***Dr. K.K.Raina****, Prof.(SPMS) & deputy director of TU and* ***Dr. Kulvir Singh****, Associate Professor and PG Incharge ,SPMS who has been a constant source of for me through out this thesis work.*

My special thank to ***Dr. Puneet Sharma*** *and* ***Ms. Loveleen brar*** *for his timely help cooperation and useful discussions during the thesis work. I wish my heartfelt thanks to research scholar* ***Ms. Kamalpreet Kuar,*** *for her guidance in whole thesis work without whom this thesis can not be completed and research scholars* ***Mr.Akshya, Mr.Vishal, Mr. Ranvir, Ms.Jashmeet, Mrs.Bhupinder and Mrs.Gurvinder*** *for their generous help and good wishes.*

My special thanks to Lab supdt.(SPMS), ***Mr. Purshottam.*** *His assistance and partnership were of great pleasure. His comments and views were very insightful and helpful..*

I am also thankfull to my friends ***Mr.Param, Mr.Pankaj, Mr.Anil, Mr.Alok, Ms.Rashmi, Ms.Rajni, Ms.Poonam, Ms. Poonam Sharma,*** *for their full cooperation, motivation and generous support. Above all render my gratitude of the ALMIGHTY who bestowed self-confidence, ability and strength in me to complete this work.*

Ramkishor

ABSTRACT

We are emphasizing our work on near eutectic Al-Si alloys. In the present study spray forming route is adopted to manufacture SiC particle reinforced LM13 alloy. Tribologic properties of these alloy under dry sliding were analyzed experimentally. Dry sliding wear behaviour of LM13 alloy and its composites reinforced with SiC particles was studied using a pin-on-disc machine. EN31 steel was used as the disc material in the wear tester. Tests were done at 50°C and 75°C temperature under the load of 2.5kg, 3.5kg and 4.5kg at a constant sliding speed of $1.6ms^{-1}$. composites exhibit better wear resistance compared to the unreinforced alloy, as-spray formed and as-cast alloy. Sn is also added in molten LM13 alloy as a microstructure modifier in different percentage.

X-ray diffraction analysis exhibited all the phases present in the spray-deposit perform. The microstructure evolution of spray cast alloy and overspray powders are discussed. Hardness of all the spray form composites and as-cast material is tested. Worn surfaces and wear debris were also examined by using SEM . Analysis of worn surfaces and wear debris indicated that dominant wear mechanisms of as-cast LM13 alloy and its composite.

CONTENTS

LIST OF SYMBOLS AND ABBREVIATIONS

MMCs	Metal Matrix Composite
^{o}C	Degree Celsius
AMMCs	Aluminium Metal Matrix Composites
AMCs	Aluminium Matrix Composite
SFAMCs	Short fibre AMCs
CFAMCs	Continuous fibre-reinforced AMCs
MFAMCs	Mono filament-reinforced AMCs
PAMCs	Particle reinforced AMCs
P/M	Powder Metallurgy
CVD	Chemical Vapour Deposition
TEC	Thermal expansion Coefficient
M.P.	Melting Point
HIP	Hot Isostatic Pressing
PVD	Physical vapor deposition
I/M	Ingot Metallurgy
CSD	Controlled Spray Deposition
ODS	Oxide Dispersion Strengthened
SD	Spray Deposition
OM	Optical Microscopy
SEM	Scanning Electron Microscopy
EDS	Energy Dispersive X-ray Spectroscopy
XRD	X-ray Diffraction

LIST OF FIGURES

LIST OF TABLES

CHAPTER - 1

INTRODUCTION

In recent years, aluminium based cast composites have gained popularity in all the emerging fields of technology owing to their superior high stiffness and strength [1]. Composites are different from metals. They are combinations of materials differing in composition or form. The constituents retain their identities in the composites and do not dissolve or otherwise merge completely into each other although they act together [2]. Reinforced concrete is an excellent example of a composite structure in which the concrete and steel still retain their identities.

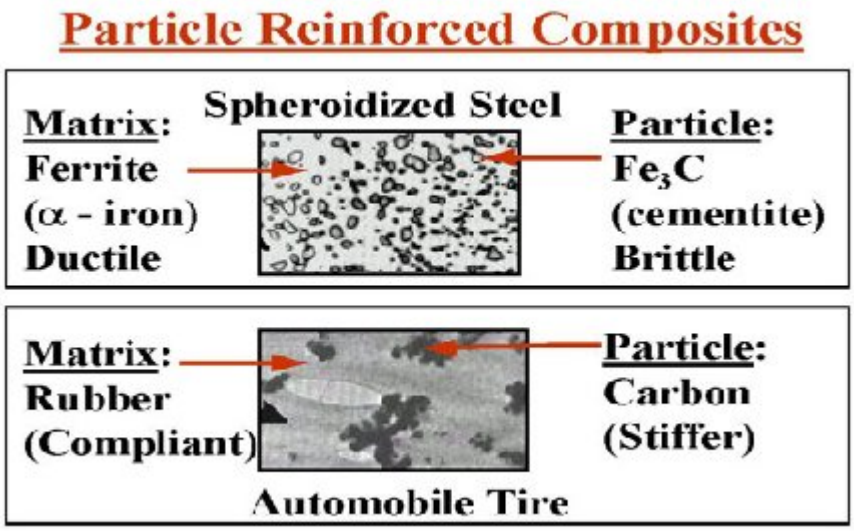

Fig.1.1 Examples for particle-reinforced composites. (Spheroidized steel and automobile tire)[3].

In an alloy matrix such type and shape of reinforcement is of great interest of present researchers to invent, develop and design a new material which have a good mechanical and other properties.

Weight reduction is the greatest advantage of composite materials and is one of the key items in decisions regarding its selection. Other advantages over conventional structure include its high corrosion resistance and resistance to damage from cyclic loading [4].

The engineered materials made from two or more constituents material which shows significantly different physical and chemical properties and which remain separate and

distinct on a macroscopic level with the finished structure is known as composite material. The composites have been proved to be one of the best selections for such materials [2].

Melt processing and powder metallurgy is the two major routes for producing particulate reinforced metal matrix composites. Compared with powder metallurgy, melt processing has some important advantages, e.g.

1) Better matrix-particle bonding,

2) Easier control of metal structure,

3) Simplicity and low cost of production [5].

Among the variety of manufacturing processes available, stir casting and spray forming, it is the commonly practiced process and advantage lies in its simplicity, flexibility and applicability to large volume production. It is also attractive because, in principle, it allows a conventional metal processing route to be used, and hence minimizing the final cost of the product. This liquid metallurgy technique is the most economical of all the available routes for metal matrix composite production, and allows very large sized components to be fabricated [6].

1.1 The most Applicable MMC

1.1.1 Aluminium matrix

Aluminium matrix composites (AMCs) have been widely studied and are now used in sporting goods, electronic packaging, armours and automotive industries. They are usually reinforced by Al_2O_3, SiC, C however SiO_2, B, BN, B_4C, AlN may also be considered as reinforcing component.[7]

(a) 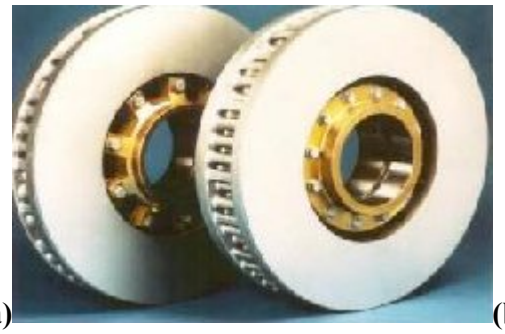 **(b)** 

Fig.1.2: Some industrial AMCs applications: (a) brake rotors for high speed train**,** (b) automotive braking systems [7].

1.1.2 Magnesium matrix

The use of magnesium alloys in car design is expanding now a days ultralight weight matrix composites are used. Typical automotive applications are engine blocks, cylinder liners, pushrods, valve spring retainers, instrument panels, clutch and brake pedal support brackets, steering column lock housings, and transmission housings[8]. Magnesium Matrix Composites are also used for manufacturing components for racing cars, lightweight automotive brake system, aircraft parts for gearboxes, transmissions, compressors and engine. Magnesium Matrix Composites are reinforced mainly by silicon carbide (SiC) particles [9].

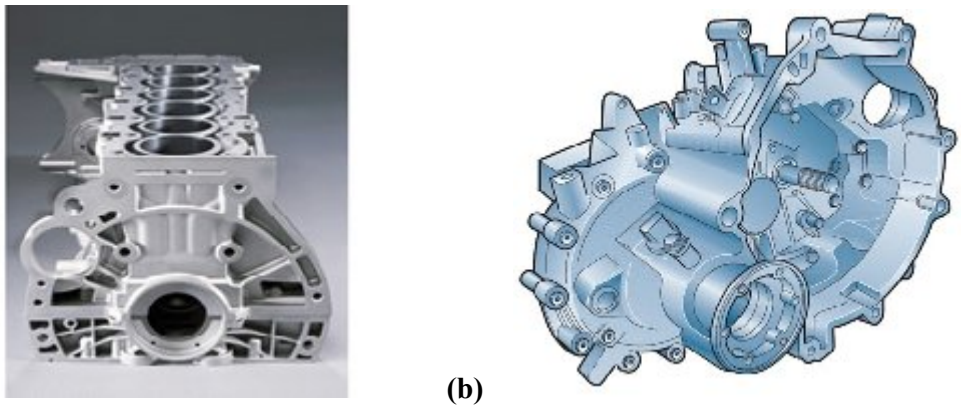

(a) **(b)**

Fig.1.3: Some Automotive MMCs applications: (a)BMW Engine block, (b) automotive gearbox [10].

1.1.3 Titanium matrix

Titanium Matrix Composites are also light weight composite, reinforced mainly by continuous monofilament silicon carbide fiber (long-fiber reinforced composites) titanium boride (TiB_2) and titanium carbide (TiC) particles (particulate composites). Titanium matrix composites are used for manufacturing structural components of the F-16 jet's landing gear, turbine engine components (fan blades, actuator pistons, synchronization rings, connecting links, shafts, discs), automotive engine components, drive train parts general machine components [9].

Fig.1.4 :Titanium Matrix Fly Eagle Jet F 16(1/8) Landinggear [11].

1.1.4 Copper matrix

Copper Matrix Composites are reinforced by continuous fibers of carbon, silicon carbon (SiC), tungsten (W), stainless steel 304 (long-fiber reinforced composites) and silicon carbide particles (particulate composites). Copper Matrix Composites are used for manufacturing hybride modules, electronic relays, electrically conducting springs and other electrical and electronic components[9].

(a)  **(b)** 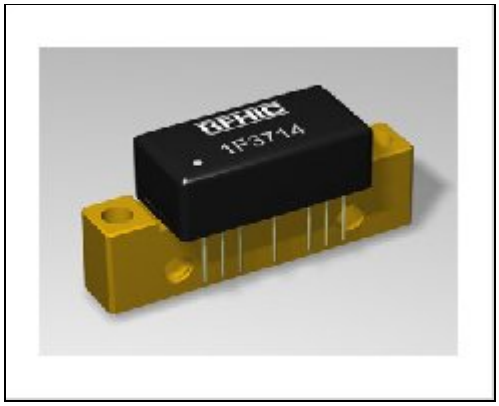

Fig.1.5: Copper matrix composite applications: (a) Electrically conducting springs[12] (b) Hybride Modules [13].

MMCs are more expensive than the more conventional materials they are replacing. As a result, they are found application where improved properties and performance can justify the added cost. Today these applications are found most often in aircraft components, space systems and high-end or "boutique" sports equipment. The scope of applications will certainly increase as manufacturing costs are reduced.

In comparison with conventional polymer matrix composites, MMCs are resistant to fire, can operate in wider range of temperatures, do not absorb moisture, have better electrical and thermal conductivity, are resistant to radiation, and do not display out gassing. On the other hand, MMCs tend to be more expensive, the fibre-reinforced materials may be difficult to fabricate, and the available experience in use is limited.

1.2 Advantages of MMCs

Compared to monolithic metals MMCs have [14]:

- Higher strength to density ratios

- Higher stiffness to density ratios
- Better fatigue resistance
- Better elevated temperature properties
- Higher strength
- Lower creep rate

1.3 Limitations of MMCs

Some of the disadvantages of MMCs compared to monolithic metals and polymer matrix composites are [14]:

- Higher cost of some material systems
- Relatively immature technology
- Complex fabrication methods for fibre-reinforced systems(except for casting)
- Limited service experience

1.4 Objectives of the present work

The present work emphasizes the literature review of Al-Si alloys and its composites. There are many manufacturing processes to form composites commercially. But the technique adopted here is rapid solidification process. The spray forming is newly developed technique and still under progress for its commercialization in developing countries like India. The objectives of present proposal are:

- To prepare the cost-effective MMC material by taking Al-Si alloy as matrix with immiscible element like Sn and also ceramic particulate like silicon carbide as reinforced phase using spray deposition technique.
- To analyze the microstructural characteristics of the as cast material.
- Hardness measurements of the as prepared MMCs.
- To study the feasibility of the material as bearing material by analyzing their wear and other related characteristics.

CHAPTER - 2

ALUMINIUM METAL MATRIX COMPOSITE

2.1 Introduction

Aluminium metal matrix composites (Al-MMCs or AMCs) are materials in which reinforcement, typically a ceramic-based material, is added with the purpose of improving the materials properties. In AMCs one of the constituent is aluminium/aluminium alloy, which forms percolating network and is termed as matrix phase. The other constituent is embedded in this aluminium/aluminium alloy matrix and serves as reinforcement, which is usually non-metallic and commonly ceramic such as SiC and Al_2O_3. Properties of AMCs can be tailored by varying the nature of constituents and their volume fraction [14].

2.2 Classification of aluminium metal-matrix composites

AMCs can be classified into four types depending on the type of reinforcement:

(a) Whisker-or short fibre-reinforced AMCs (SFAMCs)
(b) Continuous fibre-reinforced AMCs (CFAMCs)
(c) Mono filament-reinforced AMCs (MFAMCs)
(d) Particle reinforced AMCs (PAMCs)

2.2.1 Short fibre- and whisker-reinforced aluminium matrix composites (SFAMCs)

These contain reinforcements with an aspect ratio of greater than 5, but are not continuous. Short alumina fibre reinforced aluminium matrix composites is one of the first and most popular AMCs to be developed and used in pistons. These were produced by squeeze infiltration process. Fig.2.1 shows the microstructure of short fibre reinforced AMCs. Whisker reinforced composites are produced either by P/M processing or by infiltration route. Mechanical properties of whisker reinforced composites are superior compared to particle or short fibre reinforced composites. However, in the recent years usage of whiskers as reinforcements in AMCs is fading due to perceived health hazards [15] and because of this the commercial exploitation of whisker reinforced composites has been very limited. Short fibre reinforced AMCs display characteristics in between that of continuous fibre and particle reinforced AMCs.

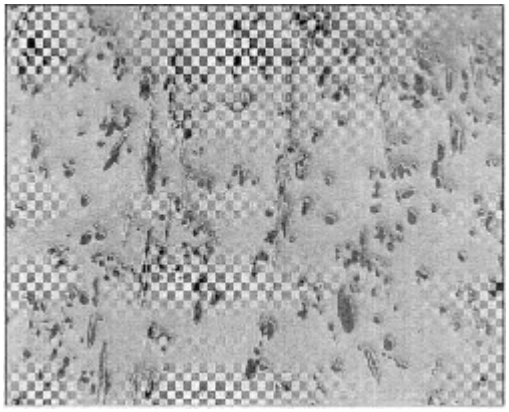

Fig. 2.1: Short fibre-reinforced aluminium matrix composite.

2.2.2 Continuous fibre-reinforced aluminium matrix composites (CFAMCs)

Here, the reinforcements are in the form of continuous fibres (of alumina, SiC or carbon) with a diameter less than 20 μm. The fibres can either be parallel or pre woven, braided prior to the production of the composite. AMCs having fibre volume fraction up to 40% are produced by squeeze infiltration technique. Alumina fibre (continuous fibre) reinforced composite having a tensile strength and elastic stiffness of 1500 MPa and 240 GPa respectively. These composites are produced by pressure infiltration route. Fig.2.2 shows the microstructure of continuous fibre (alumina) reinforced AMCs [15].

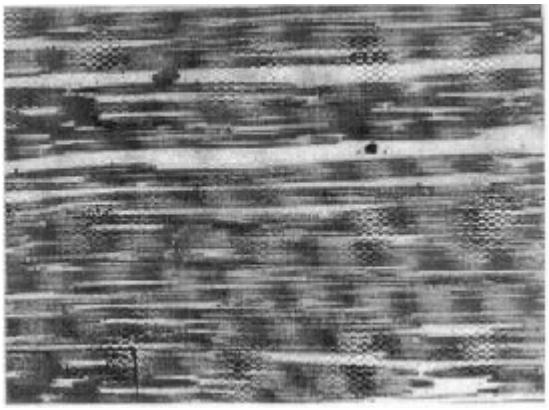

Fig.2.2: Microstructure of continuous fibre-reinforced aluminium matrix composite.

2.2.3 Mono filament reinforced aluminium matrix composites (MFAMCs)

Monofilaments are large diameter (100 to 150μm) fibres, usually produced by chemical vapour deposition (CVD) of either SiC or B into a core of carbon fibre or W wire. Bending flexibility of monofilaments is low compared to multi filaments. Monofilament reinforced aluminium matrix composites are produced by diffusion bonding techniques, and is limited to

super plastic forming aluminium alloy matrices. In CFAMCs and MFAMCs, the reinforcement is the principal load-bearing constituent and role of the aluminium matrix is to bond the reinforcement and transfer and distribute load. These composites exhibit directionality. In particle and whisker reinforced AMCs, the matrix is the major load-bearing constituent. The role of the reinforcement is to strengthen and stiffen the composite by preventing matrix deformation by mechanical restraint [15].

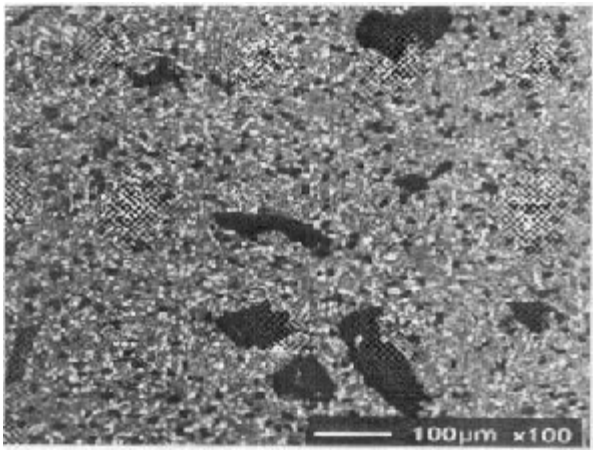

Fig.2.3: Microstructure of Hybrid composite containing 10% SiC and 4%graphit particles.

2.2.4 Particle reinforced aluminium matrix composites (PAMCs)

These composites generally contain equiaxed ceramic reinforcements with an aspect ratio less than about 5. Ceramic reinforcements are generally oxides or carbides or borides (Al_2O_3 or SiC or TiB_2) and present in volume fraction less than 30% when used for structural and wear resistance applications. However, in electronic packaging applications reinforcement volume fraction could be as high as 70%. In general, PAMCs are manufactured either by solid state (P/M processing) or liquid state (stir casting, infiltration and in-situ) processes.Fig.2.3 is the microstructure of a hybrid composite where two phases (SiC & C) is dispersed in the matrix of aluminium.

PAMCs are less expensive compared to CFAMCs. Mechanical properties of PAMCs are inferior compared to whisker/short fibre/con AMCs but far superior compared to unreinforced aluminium alloys. These composites are isotropic in nature and can be subjected to a variety of secondary forming operations including extrusion, rolling and forging. Fig.2.4

shows the microstructure of cast aluminium matrix composite having high volume fraction (40 vol%) SiC particle reinforcements[15].

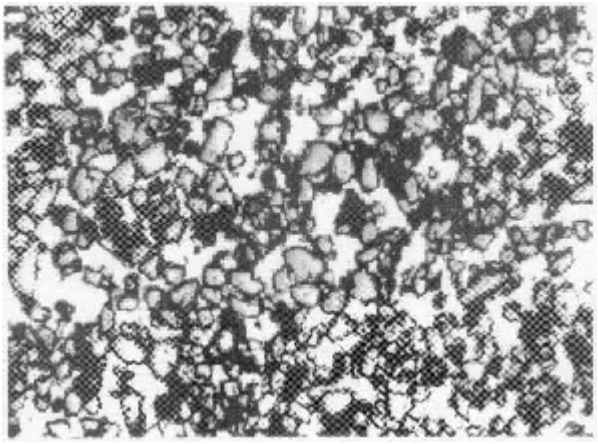

Fig2.4: Microstructures of aluminium matrix composite having high volume fraction of SiC particle reinforcement.

Table 2.1: Properties of the ceramic particulate reinforcements available [16].

Particulate type	Density (g/cm^3)	Melting point (^0C)	Modulus (GPa)	Thermal expansion Coefficient(TEC)
BORIDES				
CrB_2	5.10	2100	531	7.5
MoB	8.65	2180	324	-
TiB_2	4.50	2800	515-574	7.8
ZrB_2	6.20	3200	500-528	5.9
CARBIDES				
B_4C	2.51	2350	450	4.5
CrC	7.00	3660	370	11
SiC	3.21	2690	450	4.5
TiC	4.95	3000	460	7.6
WC	15.50	2800	700	4.9
ZrC	6.75	3500	350	6.6

NITRIDES				
AlN	3.30	2200	320	5.5
BN	3.48	2500	195	7.5
Si_3N_4	3.60	1750	300	3.7
TiN	5.50	2900	600	9.4
ZrN	7.30	3000	460	7.0
OXIDES				
Al_2O_3	3.97	2015	380	8.0
BeO	3.06	2500	380	10.3
MgO	3.75	2620	275	13.0
SiO_2	2.65	1610	110	0.55
ThO_2	9.9	3200	240	104
TiO_2	4.26	1800	88	6.8
Y_2O_3	5.01	2375	200	9.3
ZrO_2	6.27	2500	185	8.0

2.3 Silicon carbide as reinforcement

Silicon is the only chemical compound of carbon and silicon. It was originally produced by a high temperature electro-chemical reaction of sand and carbon. Silicon carbide is an excellent abrasive and has been produced and embedded into grinding wheels and other abrasive products for over one hundred years. Today the material has been developed into a high quality technical grade ceramic with very good mechanical properties. It is used in abrasives, refractories, ceramics and numerous high-performance applications. The material can also be made an electrical conductor and has applications in resistance heating, flame igniters and electronic components. Silicon carbide is composed of tetrahedral of carbon and silicon atoms with strong bonds in the crystal lattice. This produces very hard and strong material. The high thermal conductivity coupled with low thermal expansion and high strength give this material exceptional thermal shock resistant qualities. Silicon carbide ceramics with little or no grain boundary impurities maintain their strength to very high temperatures, approaching 1600^0C with no strength loss [17].

Properties

- Low density

- High strength
- Low thermal expansion
- High thermal conductivity
- High hardness
- High elastic modulus
- Excellent thermal shock resistance
- Superior chemical inertness

SiC particles were more effective than Al_2O_3 particles of wear resistance of Al matrix composites due to the high hardness. An increase in the weight percentage of SiC particulates along the deposition direction led to a progressive increase in the porosity levels and matrix hardness for Al/SiC_p and Al-Si/SiC_p [19].

Table 2.2: Properties of Silicon carbide.

Properties	Silicon carbide
M.P.(^{0}C)	2200-2700
Limit of applications(^{0}C)	1400-1700
Hardness(Mohr's Scale)	9
Density(g/cm^3)	3.2
Linear coeff. of expansion(10^{-6} K)	4.5
Fracture toughness (MPa- m$^{1/2}$)	4.6
Crystal structure	hexagonal

Matrix reinforced with two or more reinforcement types is known as hybrid composite. Song et al. successfully fabricated Al/Al_2O_3/C hybrid metal composite by squeeze casting method. The wear resistance of hybrid composites of alumina and carbon fibres indicates more effectiveness than that in the composites reinforced with alumina fibres, Jinhai Gu et al. synthesized 6061/Al/SiC_p/Gr hybrid composite by spray atomization and deposition. The aim of this work is to improve mechanical properties of the material by introducing SiC_p and graphite for damping property[20].

2.4 Bonding and interface formation in metal matrix composite

Metal matrix composites consist of an intricate structure of metals and a ceramic reinforcing material. The frontier zone between these two phases (i.e. interface or interphase) is one essential part of MMC. Bonding develops from physical or chemical interactions, interfacial

frictional stress and thermal stresses due to mismatch between coefficient of thermal expansion of reinforcement and matrix. The understanding and control of the underlying interfacial phenomena governing the transmission of thermal, electrical, and mechanical properties across the whole composite might become of paramount importance when designing MMC for a particular task [22].

2.4.1 Interfacial characteristics in MMCs

The interfacial problematic in MMC has been studied physical and chemical properties of both the matrix and the reinforcement material, the actual strength and toughness desired for the final MMC, a compromise has to be achieved balancing often several conflicting requirements. In the case of continuous fibre reinforced metals (CFRM) high strength is achieved by preventing chemical reactions between the matrix and the inorganic fibres. While a weak interface is desirable to enhance longitudinal strength and toughness, a strong interface is desirable to achieve good transverse properties in CFRM. A weak interface will lead crack propagation following the interface, while a strong matrix associated with a strong interface will reveal cracks across both the matrix and the reinforcements. However, the matrix is weak in comparison with both the interface and the particle strength, the failure will propagate through the matrix itself [23].

2.4.2 Physical phenomena present at the interface

The wettability of the reinforcement material by the liquid metallic matrix plays a major role in the bonding formation. It mainly depends on heat of formation, electronic structure of the reinforcement and the molten metal, temperature, time, atmosphere, roughness and crystallography of the reinforcment. Fig.2.5 shown below illustrates the degrees of wetting and corressponding contact angles.

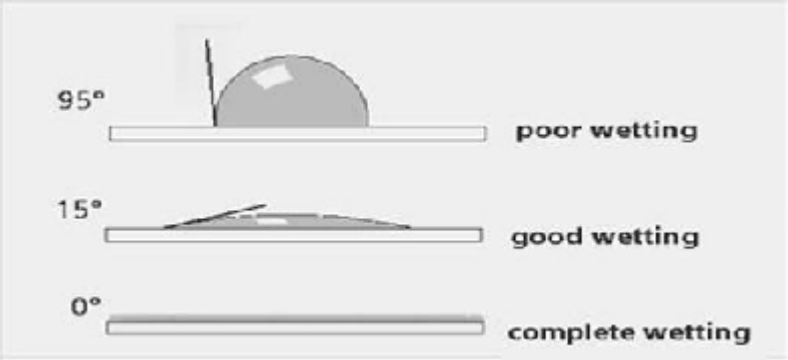

Fig. 2.5: Sketch of three degrees of wetting and the corresponding contact angles.

Wettability can be defined as the ability of a liquid to spread on a solid surface. It also describes the extent of intimate contact between a liquid and a solid. Successful incorporation of solid ceramic particles into casting requires that the melt should wet the solid ceramic phase. The basic means used to improve wetting are:

(a) Increasing the surface energies of the solid,
(b) Decreasing the surface tension of the of the liquid matrix alloy,
(c) Decreasing the solid-liquid interfacial energy at the particles-matrix [24].

Similarity between metallic and covalent bonding is reflected in that some metal-like solids (TiC, ZrC) are more easily wetted than strongly ionic ceramics such as alumina that remains poorly wetted. Surface roughness of the reinforcing material improves the mechanical interlocking at the interface, though the contribution of the resulting interfacial shear strength is secondary compared to chemical bonding. Large differences in thermal expansion coefficient between the matrix and the reinforcement should be avoided as they can induce internal matrix stresses and ultimately give rise to interfacial failures [23].

In some cases, such as for Al-SiC, the reactivity even persists below the solidus line. The chemical processes involved here are the oxidation of one element from the matrix and the reduction the reinforcing materials. Though thermodynamically favoured, some reactions are however not observed and practically the kinetics of these reactions has to be considered in conjunction with thermodynamic data in order to evaluate the real potential of the reactions.

2.4.3 Metallurgy of the interfacial area

The MMC requires often a very short solidification time to avoid excess interfacial reaction. During the cooling process, differences in thermal capacity and conductivity between the reinforcing material and the matrix induce localised temperature gradients. Solidification of the metallic matrix is believed to be generally a directional outward process, starting from the inside of the metallic matrix while ending at the reinforcing material surface. Whereas this problem is mostly limited to few insoluble impurities (Fe, Si) been carried to the interface for single metal systems, heterogeneities such as insoluble precipitates or enriched phases are often found concentrated at the interface and grain boundaries when working with alloys (Cu, Si containing Al alloys). Depending on the alloy undesired phases can be dissolved by a subsequent heat treatment[25].

In addition, the surface tension of the molten metal can be reduced by traces of alloying elements. Such effects has been reported for aluminium using Pb, Sn, Mg, and Sr. Finally the processing type and parameters have to be selected and adjusted to a particular MMC system [26].

Metals are generally more reactive in the liquid rather than in the solid state. Consequently short processing times, i.e. short contact times between the liquid metal and the reinforcement can limit the extend of interfacial reactions. For instance, Al-SiC MMC free of interfacial aluminium carbide can be processed in few seconds by squeeze casting without the need of saturating the matrix with Si. It is worth noting here that solid state processing such as powder metallurgy precludes liquid phase reactions but also it allows more flexibility in terms of MMC-systems, it remains mainly limited to particulate reinforcements [27].

2.5 Mechanical properties of AMMCs

2.5.1 Wear property

Wear is the loss of material from a surface by means of some mechanical action. The mechanism of wear is very complex. It should be understood that the real area of contact between two solid surfaces compared with the apparent area of contact is invariably very small, being limited the points of contact between surfaces. The load applied to the surfaces will be transferred through these points of contact and the localised forces can be very large. The material intrinsic surface properties such as hardness, strength, ductility, work hardening etc. are very important factors for wear resistance, but other factors like surface finish, lubrication, load, speed, corrosion, temperature and properties of the opposing surface etc. are equally important [5].

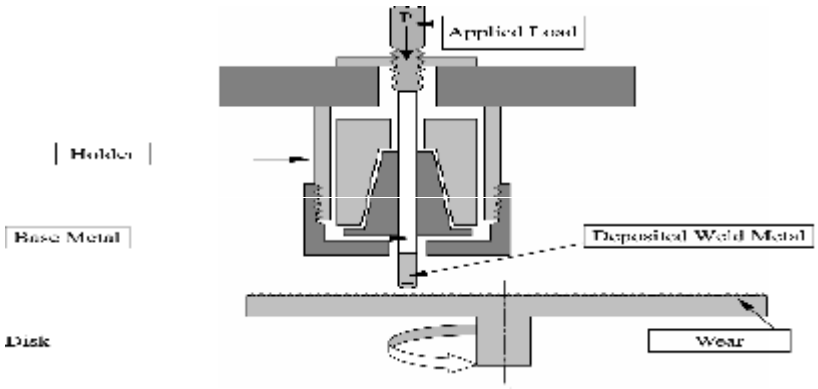

Fig2.6: Wear testing (Pin-on-disc machine)

2.5.1.1 Adhesive wear

Adhesive wear is defined as the transfer of material from one surface to another during relative motion by a process of solid-phase welding or as a result of localised bonding between contacting surfaces. Particles that are removed from one surface are either permanently or temporarily attached to the other surface [5].

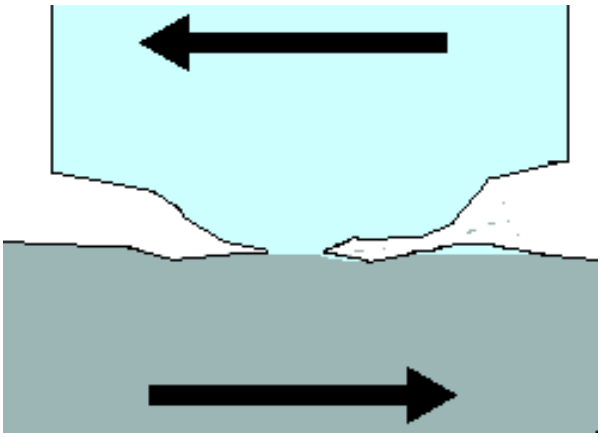

Fig.2.7: Adhesive wear

2.5.1.2 Delamination wear theory

Suh[28] proposed that at low sliding speeds, wear debris formation could be described by a delamination wear theory. Wear processes such as adhesive wear, fretting and fatigue were all related to this same mechanism. Suh[28] stated that wear occurred by the following sequential steps:

- Cyclic plastic deformation of surfaces layers by normal and tangential loads.
- Crack or void nucleation in the deformed layers at inclusions or second-phase particles.
- Crack growth nearly parallel to the surface.
- Formation of thin, long wear debris particles and their removal by extension of cracks to the surface.

Al-Si alloys which are used for structural purposes have wide range of composition which varies from hypoeutectic to hypereutectic compositions. However, eutectic and near eutectic Al-Si alloys with Si contents (≈12.6 wt% Si) exhibit desirable physical properties.

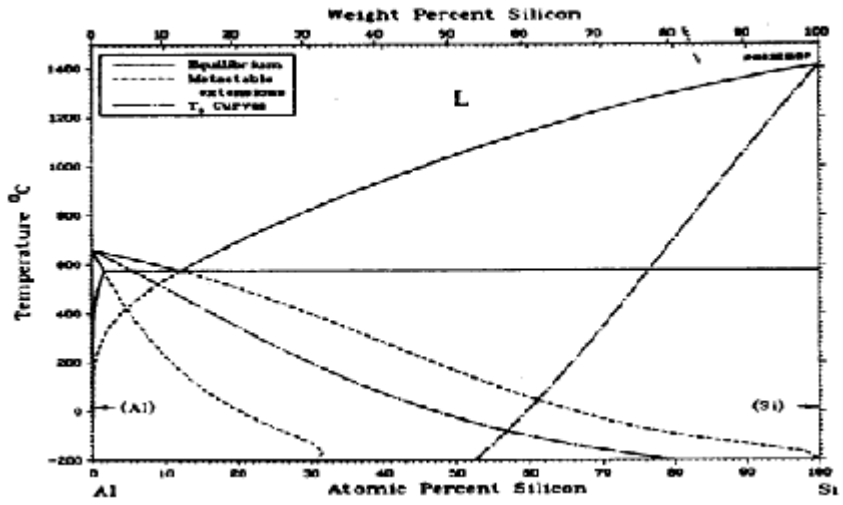

Fig.2.8: Phase diagram for the Al-Si system showing metastable extensions of liquidus and solidus lines.

2.5.2 **Hardness test**

Hardness is the property of a material that enables it to resist plastic deformation, usually by penetration. However, the term hardness may also refer to resistance to bending, scratching, abrasion or cutting.

Hardness of materials has probably long been assessed by resistance to scratching or cutting. An example would be material B scratches material C, but not material A. Alternatively, material A scratches material B slightly and scratches material C heavily. Relative hardness of minerals can be assessed by reference to the Mohs scale that ranks the ability of materials to resist scratching by another material. Similar methods of relative hardness assessment are still commonly used today. An example is the file test where a file tempered to a desired hardness is rubbed on the test material surface. If the file slides without biting or marking the surface, the test material would be considered harder than the file. If the file bites or marks the surface, the test material would be considered softer than the file [29].

There are different type of hardness testing methods are available. Rockwell hardness test, brinell hardness test, Vickers hardness test and microhardness test are the most applicable hardness testing methods. In this testing technique different types of ball and load are used for different materials. The diameter of ball and applied load is depend upon the material type.

2.6 Processing techniques

MMC manufacturing can be broken into three types:

1) Solid State Processing

2)Liquid State Processing

3)Vapor Deposition [14, 28, 29]

2.6.1 Solid state methods

- *Powder blending and consolidation (powder metallurgy):* Powdered metal and discontinuous reinforcement are mixed and then bonded through a process of compaction, degassing, and thermo-mechanical treatment (possibly via hot isostatic pressing (HIP) or extrusion).
- *Foil diffusion bonding*: Layers of metal foil are sandwiched with long fibers, and then pressed through to form a matrix.

2.6.2 Liquid state methods

- *Electroplating / Electroforming*: A solution containing metal ions loaded with reinforcing particles is co-deposited forming a composite material.
- *Stir casting*: Discontinuous reinforcement is stirred into molten metal, which is allowed to solidify.
- *Squeeze casting*: Molten metal is injected into a form with fibers preplaced inside it.
- *Spray deposition*: Molten metal is sprayed onto a continuous fiber substrate.
- *Reactive processing*: A chemical reaction occurs, with one of the reactants forming the matrix and the other the reinforcement.

2.6.3 Vapor deposition

- *Physical vapor deposition*: The fibre is passed through a thick cloud of vaporized metal, coating it.

2.6.4 In-situ fabrication technique

Controlled unidirectional solidification of a eutectic alloy can result in a two-phase icrostructure with one of the phases, present in lamellar or fiber form, distributed in the matrix [28, 29].

2.6.5 Most common processing techniques for manufacturing of AMMCs

1) Powder Metallurgy(P/M)
2) Stir Casting
3) Spray forming

2.6.5.1 Powder metallurgy for aluminium matrix composite

Among all the metal matrix composites (MMCs) aluminium could be the most widely used metal as matrix due to its low density coupled with high stiffness. There are different manufacturing methods which can be applied for this composite. From these, P/M could be remarked as a highly effective and economic method compared with other alternatives[30].

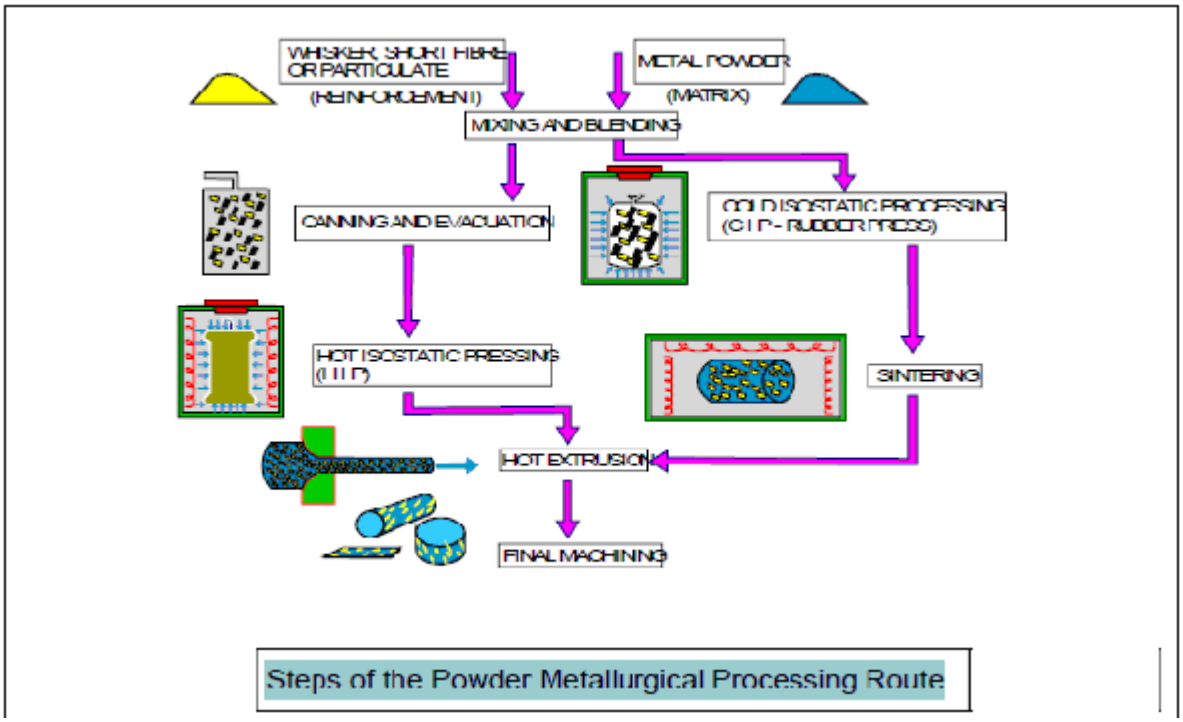

Fig. 2.9: Steps of the powder metallurgical processing route [30].

2.6.5.2 Production of powder of metals

Almost all metals and their alloys can be converted into powder form. Metal powders are commonly produced by atomization techniques. A stream of molten metal is disrupted either by impacting another fluid (gas or water) jet under high pressure or by applying mechanical forces and electrical fields leading to formation of fine liquid metal droplets which then solidify resulting in fine powder particles. The inert gases, argon and nitrogen, are used in the gas atomization, and the resulting powder particles are smooth and spherical with 50-100 micro meter diameter. The impact of very high intensity gas pulse waves in supersonic and ultrasonic gas atomization can lower particle sizes to 10μm [30, 31].

2.6.5.3 Mixing of matrix metal powder and ceramic particulates

There are quite a few composite fabrication techniques using continuous fibres of which two processes that use hot pressure bonding need special mention. In one process (known as powder cloth process), metal powder filled clothes are first produced by mixing metal matrix powders with an organic binder and then blending with a high purity Stoddard solution. On application of low heat, the Stoddard solution evaporates leaving behind a dough-like mixture which, on rolling, yields a metal powder cloth. Alternate layers of powder clothes and fibre mats, when hot press bonded, form a composite laminate. The binders usually burn out without leaving any residue.

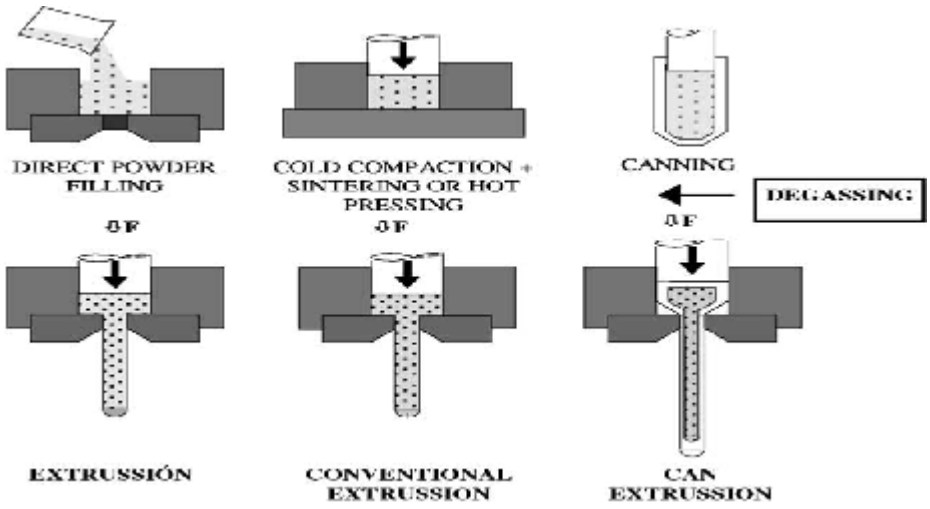

Fig.2.10: Powder metallurgy extrusion process [32].

When the reinforcements are in the form of short fibres and particulates, metal matrix powder and reinforcements are thoroughly blended, and the blend is degassed to remove volatiles and then a composite ingot is formed by either hot pressing in vacuum or hot isostatic pressing. The composite ingot is subsequently used to fabricate structural components using secondary fabrication processes. Major problems are encountered in controlling the shape, size and distribution of reinforcements in the matrix. The alignment of short fibres, elongation of particulates i.e., a sphere changing to an oblate or nonspherical shape, and uniform dispersion or clustering are the common occurrences that influence the microstructure of the composite [31].

2.6.5.4 Properties of P/M aluminium matrix composites

In general, P/M aluminium matrix composites exhibit good levels of mechanical properties compared to those from other alternative manufacturing processes. In case of an Al matrix, this can be increased to more than 200 MPa in tensile strength by short periods of holding time at 300°C [33]. Longer periods can produce the appearance of dimensional instabilities. P/M is one of the most widely used methods for producing aluminium matrix composites due to its low processing costs added to its high versatility. On the other hand, some types of composites cannot be made by any other alternative route. Aluminium alloys offer a combination of mechanical and tribological properties and low density that makes them highly suitable for composite manufacturing that can be used in several industries. The widely used particle reinforcements are SiC, Al2O3 and recently different system of intermetallics [32].

2.6.5.5 Advantages of powder metallurgy for part production

The technical and commercial advantages of producing parts from powder can be summarised as below:

- production to near-net shape
- few or no secondary operations
- high material utilisation from low levels of ‘in process scrap’
- homogeneous powder, and hence part, chemical composition due to absence of gross
- solidification segregation and uniform pre-alloyed powder particle composition

- ❖ unique compositions and structures possible as there is no melting e.g. introduction of
- ❖ specific particles to give special properties such as silica and graphite in brake pads, and
- ❖ porosity in bearings for oil retention
- ❖ non-equilibrium compositions possible e.g. copper-chromium alloys
- ❖ metallurgical structures are usually fine and isotropic e.g. carbide distribution in
- ❖ atomised high speed steel powder parts [34].

2.6.5.6 Disadvantages and limitations of powder metallurgy for part production

- ❖ costs of powder production
- ❖ limitations on the shapes and features which can be generated e.g. the process cannot
- ❖ produce re-entrant angles by fixed die pressing or radial holes in vertically pressed cylinders
- ❖ the size will always change on sintering. This can usually be predicted as it depends on number of factors including 'as-pressed' density which can be controlled potential workforce health problems from atmospheric contamination of the workplace [34].

2.6.6 Stir casting process for producing aluminium matrix composite

Stir casting is a liquid state method of composite materials fabrication, in which a dispersed phase (ceramic particles, short fibers) is mixed with a molten matrix metal by means of mechanical stirring. Stir casting is the simplest and the most cost effective method of liquid state fabrication. The liquid composite material is then cast by conventional casting methods and may also be processed by conventional metal forming technologies [35].

In general stir casting of MMC involves producing a melt of selected matrix material followed by the introduction of reinforcement material into the melt and the dispersion of the reinforcing material through stirring. Stirring is carried out vigorously to form a vortex where the reinforcing particles are introduced through the side of the vortex. The formation of the vortex will drag not only the reinforcement particles into the melt, but also all impurities

which are formed on the surface of the melt. The vortex will also entrap air into the mould which is extremely difficult to remove as the viscosity of the slurry increase [36].

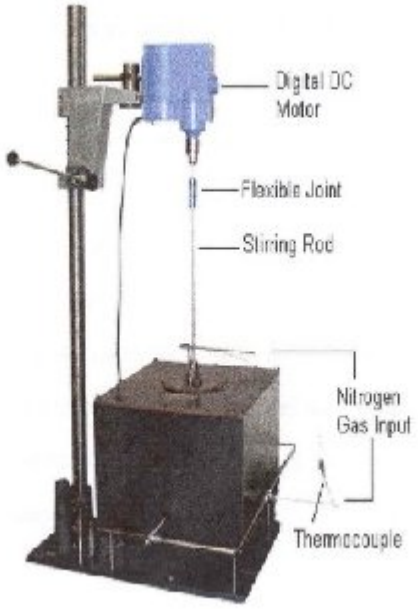

Fig.2.11: Stir Casting Process

Here, ceramic particles are incorporated into the alloy in the solid state Stir casting set-up mainly consists a furnace and a stirring assembly (Fig.2.11).In general, the solidification synthesis of metal matrix composites involves producing a melt of the selected matrix material followed by the introduction of a reinforcement material into the melt, obtaining a suitable dispersion. The next step is the solidification of the melt containing suspended dispersoids under selected conditions to obtain the desired distribution of the dispersed phase in the cast matrix [15].

2.6.7 Spray forming process for producing aluminium matrix composite:

Spray forming is a metallurgical process that combines the main advantages of the two classical approaches to base manufacturing of sophisticated material and performs, i.e.:

1) *Metal Casting*: involving high-volume production and near-net shape forming.

2) *Powder Metallurgy*: involving near-net shape forming at small volumes to yield a homogeneous, fine-grained microstructure.

The spray forming process essentially combines atomization and spraying of a metal melt with the consolidation and compaction of the sprayed mass on a substrate [37].

Spray forming is a unique solidification process in which metal melt is atomised by inert gas into droplets of 10-200 microns in size, flying at subsonic speed onto a deposition substrate shows in Fig.1.17. During the flight the droplets are rapidly cooled with a cooling rate between 100 to 100,000 degrees per second in a controlled way so that the solidification of the metal is not dependent on the temperature and/or the thermal properties of the deposition surface like a mould. The particles arriving at the mould are in such a condition that welding to the already deposited metal is complete and no interparticle boundaries are developed. As a result, high-quality materials are made with fine, equiaxed and homogeneous microstructures. These features are especially prominent in making high-alloy metal components like for example die inserts and tooling heads[38].

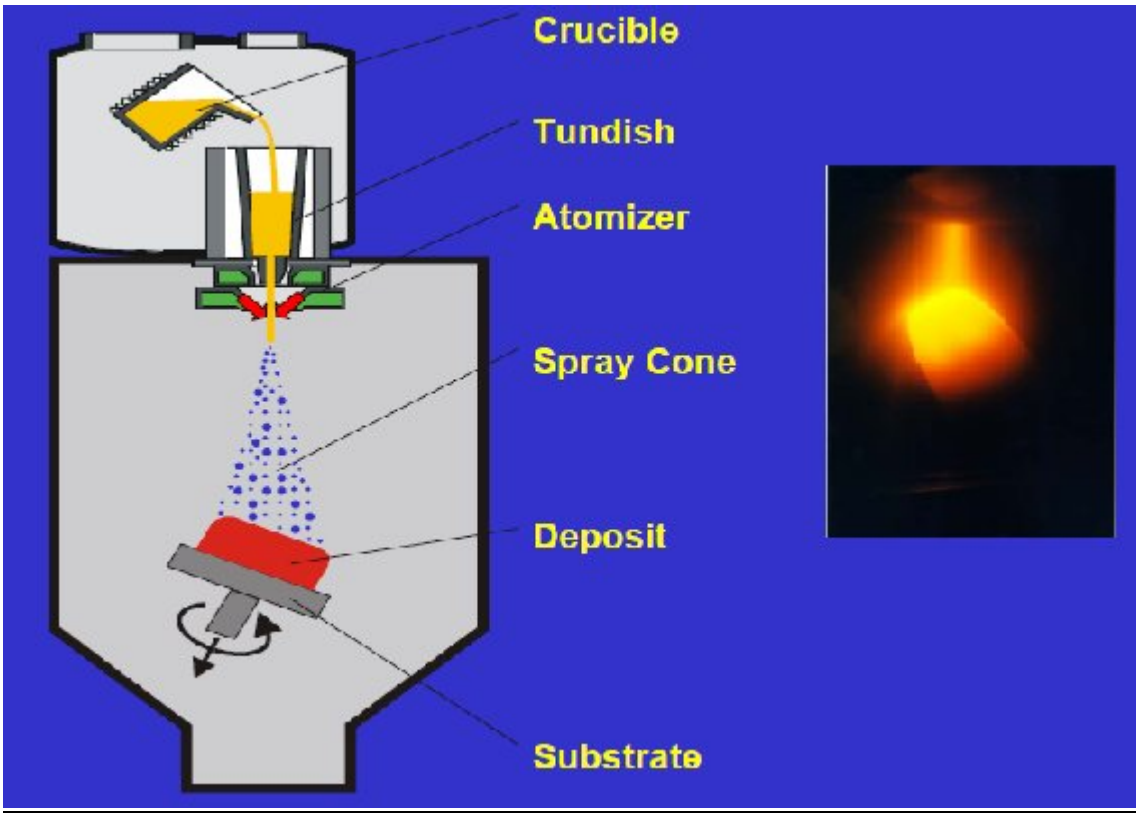

Fig.2.12: Illustration of Spray forming process [39].

Generally, spray formed alloys show the following characteristics:

1) High-density preforms, typically 96-99% of theoretical, are produced.
2) Oxygen content is decreased, compared to P/M products, and degassing operations are not needed.
3) Rapid solidification results in a fine, uniform grain size, typically in the range 20-50 μm.
4) As a result of rapid solidification, macrosegregation is sharply decreased.
5) Fine precipitates are produced and uniformly distributed in the microstructure. Although precipitation in the liquidus/solidus region occurs very rapidly, any solid-state transformations are relatively slow.
6) Superior fracture properties are obtained in comparison to P/M and I/M products. There are two reasons for this:
    i) Decreased oxidation compared to P/M;
    ii) Absence of coarse precipitates compared to I/M [40].

The schematic diagram of reinforcement of particulates in a spray forming set up is as shown in Fig.2.13. The particulates can be either incorporated in atomization zone (Fig.2.13a) or during melting the alloy (Fig.2.13b) in furnace as done in stir cast process. The basic parts of it are a metal melting unit or a furnace, a gas atomizing unit and a preform unit. A metal melting unit is basically a furnace used for melting alloys ranging from aluminium to steel and cast iron. It is fitted with a nozzle through which metal will be sprayed.

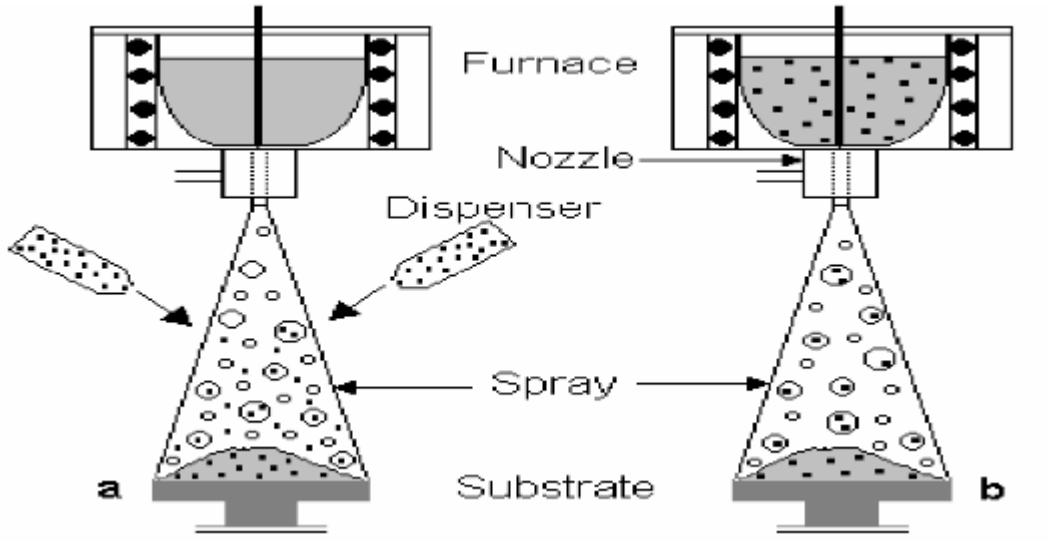

Fig. 2.13: Mode of Particle Addition in Co-Spray Deposition Technique [39].

2.6.7.1 Development of spray casting

The principles of the spray deposition process were developed by Singer at the University of Swansea in the early 1970s[41]. Singer suggested the production of rolling strip directly from molten metal as an alternative to the practice of casting and rolling large ingots. The spray rolling of metals studied by Singer became an alternative to a process originally developed at the Reynolds Metal Company in 1967 in which aluminium was centrifugally atomised, reheated, fed into roll gaps, and hot rolled to produce strip in a continuous operation. Most of Singer's work was performed on aluminium alloys. The general principle of Singer's process was to atomise a stream of molten aluminium alloy using nitrogen and to direct the resulting spray on to a pair of rolls. However, during this process, the thickness of the as-deposited strip was not uniform across its width [42].

Several years later, Osprey Metals Ltd., UK, which was set up as a commercial enterprise by G. Brooks, A. Leatham, and J. Combs, all graduate students from Swansea, utilised the early ideas of Singer, for the production of forging preform.

The Osprey process became an alternative to the existing two basic production methods; the forging of pre-rolled material and the powder metallurgy route. The first method involves melting, casting into ingots, rolling into bar, cutting into slugs, reheating and then forging. This was the most common method for the production of forgings. However, this route was expensive, because of the large quantities of scrap generated. Powder metallurgical routes, which require many process stages consisting of atomisation, sieving, blending, de-gassing, compacting, heating and then forging, is also expensive. The Osprey process, which offers significant economic and technical benefits to the forging industry, resulted in two patents awarded to Brooks.

In 1980, the application of the principles of spray deposition to highly alloyed tool and high-speed steels was developed by Aurora Steels Ltd. This work resulted in the technique known as controlled spray deposition (CSD) which consisted of atomising a stream of molten metal and projecting the high velocity liquid droplets so that they collided with a cool substrate. This process was based on the Osprey Process and used coarse (0.5-1.5 mm) liquid droplets [43].

On impact, the droplets splatted achieving cooling rates of 103 Ks^{-1}. In 1983, Aurora Steels closed the majority of its operations due to the economic recession in the UK. Subsequent studies based on the spray forming process resulted in the development of the liquid dynamic

compaction (LDC) process. In this process, high gas pressure was employed under a tightly controlled atmosphere to generate fine, rapidly quenched droplets [44].

2.6.7.2 Steps in spray forming

Atomization

Atomization was derived from the use of powder metallurgy processing. Atomization is the most critical step in spray deposition processing, since our ability to excise a large degree of process control is intimately linked to the mechanism that govern droplet generation. The atomization technology that is frequently used in spray deposition processing is adopted from conventional powder atomization practices. In powder metallurgy atomization is used to produce fine metal powders. In most cases , atomization involves the impingement of a liquid stream by a high velocity fluid, which may be either gas or liquid. In the process of atomization droplets of molten metal are produced and eventually solidify. Atomization processes can be classified into the following major categories:

a) Pressure atomization
b) Air (air-spray) atomization
c) Centrifugal atomization

a) Pressure atomization

In the airless atomization process, high pressure forces fluid through a small nozzle. The fluid emerges as a solid stream or sheet at a high speed. The friction between the fluid and the air disrupts the stream, breaking it into fragments initially and ultimately into droplets. The energy source for this form of atomization is fluid pressure, which is converted to momentum as the fluid leaves the nozzle.

Three factors that affect an airless spray include the atomizer orifice diameter, the atmosphere, and the relative velocity between the fluid and the air. Regarding orifice diameter, the general rule is that the larger the diameter or size of the atomizer orifice, the larger the average droplet size in a spray.

Fig.2.13: Airless atomization with fluid under pressure.

The atmosphere provides resistance and tends to break up the stream of fluid. This resistance tends to overcome, in part, the fluid's properties of surface tension, viscosity, and density. In addition, the air temperature may also affect atomization.

The relative velocity between the fluid and the air also affects droplet sizes. The fluid's velocity is created by pressure in the nozzle. As the fluid pressure increases, velocity increases and the average droplet size decreases. And conversely, as fluid pressure decreases, velocity is lower and the average droplet size is larger [46].

b) Air-spray atomization

In air-spray atomization, fluid emerging from a nozzle at low speed is surrounded by a high speed stream of air. Friction between the liquid and air accelerates and disrupts the fluid stream and causes atomization. The energy source for air atomization is air pressure. The operator can regulate the flow rate of fluid independently of the energy source. Fig.2.14 illustrates a stream of fluid passing through an orifice; as it emerges, a high speed stream of air surrounds the fluid stream [46].

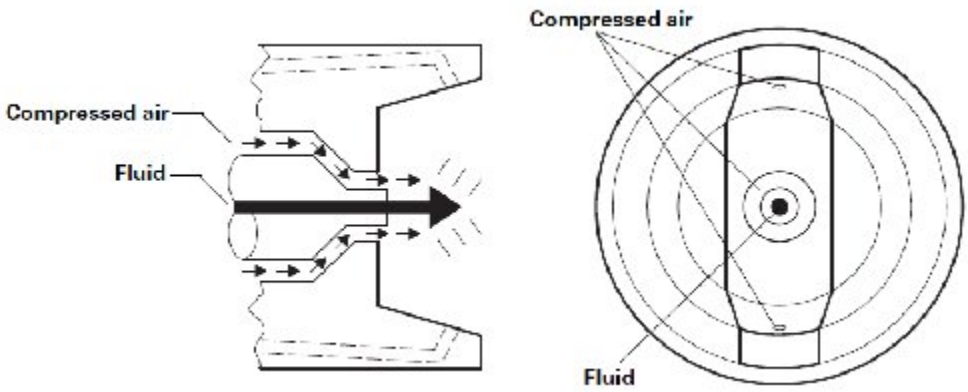

Fig2.14: Air-spray atomization with high velocity air

c) Centrifugal atomization

In centrifugal or rotary atomization, a nozzle introduces fluid at the center of a spinning cup or disk. Centrifugal force carries the fluid to the edge of the disk and throws the fluid off the edge. The liquid forms ligaments or sheets that break into fine droplets. Fig.2.15 shows the mechanism of centrifugal atomization. The energy source for rotary atomization is centrifugal force. With the same rotational speed, at low flow rates, droplets form closer to the edge of the disk than with higher flow rates. The spray pattern tends to move radially away from the disk or cup in all directions (360°). With rotary atomization, operators can control both the

flow rate and the disk speed independently of each other. In most spray coating rotary applications, electrostatic charge is applied to the spray to attract the droplets to a grounded target object. In some types of atomizers, such as bells, shaping air can be added to move the spray forward in an axial direction [46].

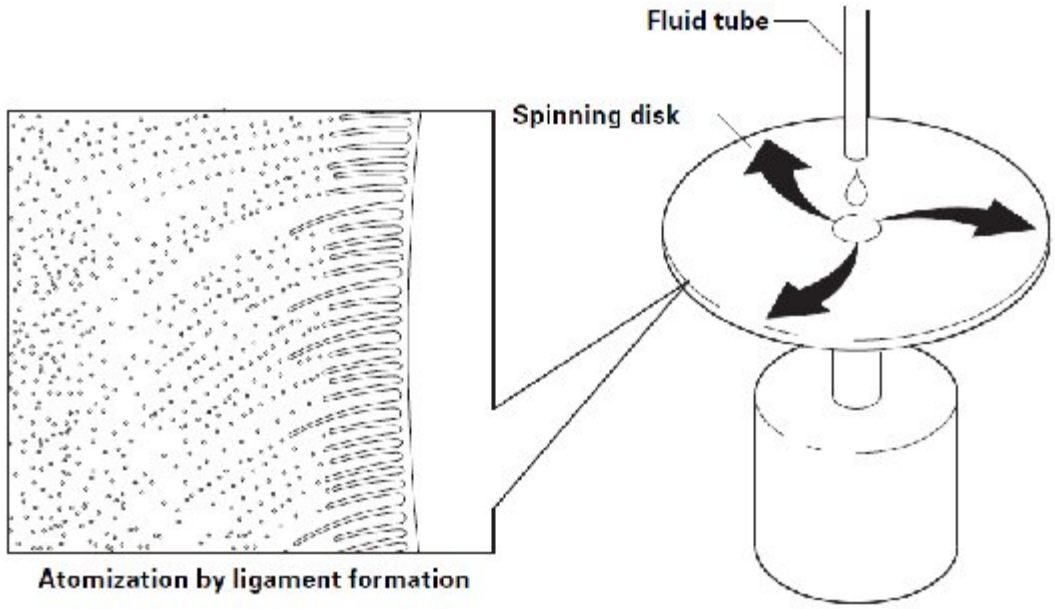

Fig2.15: Centrifugal atomization process.

Centrifugal atomization involves pouring molten metal at relatively low flow rates (0.1-2kg/min) onto a spinning plate, dish or disc as shown in Fig.2.15. The rotation speed of plate is sufficient to create high centrifugal forces at the periphery and overcome surface tension and viscous forces so the melt is fragmented into droplets. Droplet diameters produced by centrifugal atomization are dependent primarily on the rotation speed, (up to 20,000rpm) and are typically in the range 20 – 1000 μm with cooling rates of the order 10^4 Ks^{-1}) . Centrifugal atomization is generally conducted under an inert atmosphere of Ar or N_2 to prevent oxidation of the fine droplets or can be operated under vacuum [46].

The gas assisted spray forming processes are the most well developed, attracting world-wide interest for the processing of Al, Ni and Fe based alloys. The process is economically constrained by the post-spray processing problems due to gas entrapment and thermal induced porosity in the product.

2.6.7.3 Atomizer designs

The atomiser design plays an important role in the atomisation of the molten metal stream. The design of atomisation nozzle, which changes the potential energy of the gas into kinetic energy, controls the size of droplets. There are two types of nozzle design, namely free fall and close-coupled, as shown in Fig.2.14 In the free fall design, after travelling a relatively large distance, the gas interacts with the melt stream about 5 to 30 cm before impact. Therefore, the gas velocity decreases whilst travelling between the nozzle exit and the point of impact. This results in insufficient atomisation and large sized droplets in the spray. In the close-coupled design, the gas strikes the metal stream at the end of the melt delivery tube. This results in a highly efficient energy transfer from gas to metal, leading to fine droplets in the spray. This is because of the shorter distance between the gas and metal stream before they interact.[48]

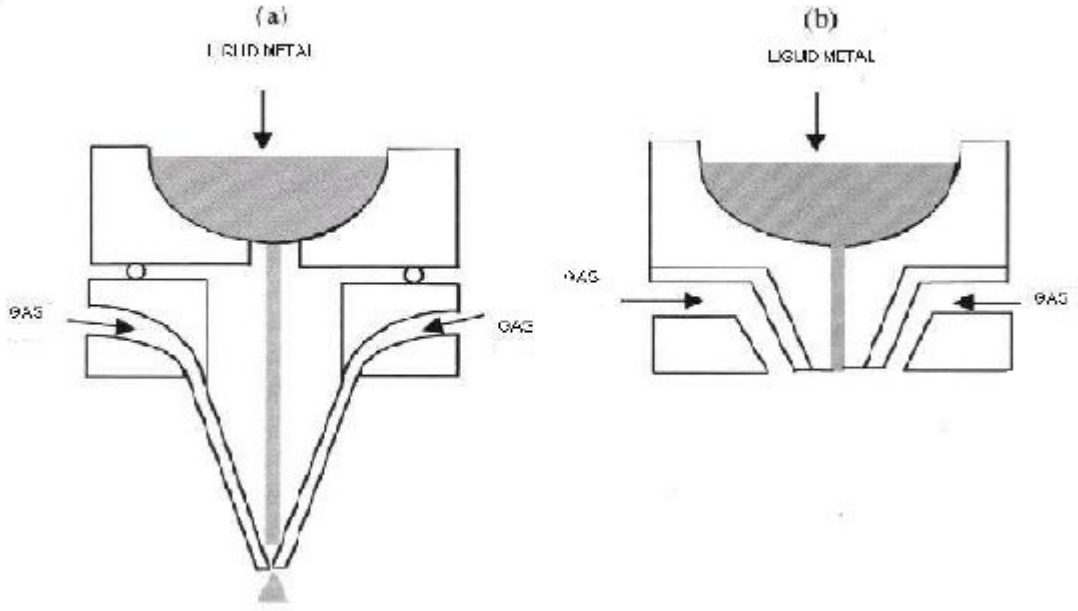

Fig2.14: Diagram showing typical nozzle designs used in spray generation (a) free fall (b) close-coupled

Here, two kinds of gas atomizer, as shown schematically in Fig. 2.14(a) and Fig. 2.14(b). In free fall or open atomizers in Fig. 2.14(a), the melt falls unconstrained into a region where atomization occurs. In close coupled or closed atomizers in Fig. 2.14(b), the gas atomizes the metal directly on exit from the melt delivery nozzle. The gas kinetic energy is consequently higher in comparison with open atomizers and gives smaller median diameters. However because the tip of the melt delivery nozzle is chilled by the flow of the cool atomizing gas in

closed atomizers, freezing of the metal may occur before atomization (freeze off) and closed designs are generally only used in conjunction with low melting point materials where the temperature difference between melt and gas is relatively small [48].

Secondary gas jets may be used either to shroud the molten metal stream prior to atomization or to restrict spray divergence of the droplet spray after atomization. Droplet spray scanning is used to average spatial variations in spray density and droplet size over the preform surface and allow large diameter preforms (up to 350 mm) to be manufactured. Scanning is achieved either by an alternating gas flow from opposing jets (Fig.2.15a) or by mechanical oscillations of the atomizer (Fig.2.15b).

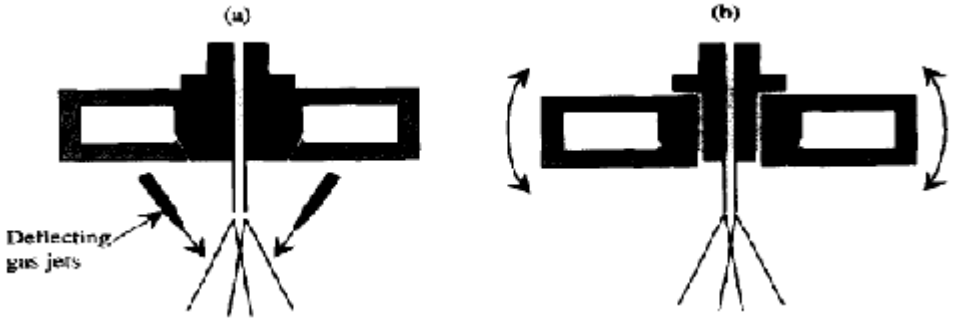

Fig.2.15: Schematic of (a) pneumatic and (b) mechanical scanning atomizer arrangement [2].

Spray deflections of 5-10° at frequencies of up to 25 Hz are achievable. For larger preform diameters up to 450 mm where the required spray scan angle and corresponding changes in preform/atomizer separation become too large, twin or multi-atomizers simultaneously spraying onto a single preform have been suggested.

Atomizing gas used in spray forming is generally either N_2 and can be either protective or reactive depending on the alloy system, or Ar which is generally entirely inert but more expensive than N_2. Reactive gasses can be introduced in small quantities to the atomizing gas to create dispersion strengthened alloys e.g. 0.5–10 % O_2 in N_2 used to generate oxide dispersion strengthened (ODS) Al alloys. Comparisons of N_2 and Ar based spray forming showed that with all other factors remaining constant, the billet top temperature was lower with N_2 than with Ar, because of the differences in thermal diffusivity of the two atomizing gases: Ar has a thermal conductivity of 0.0179 W/mK which is approximately a third less than N_2 with a thermal conductivity of 0.026 W/mK.

2.6.7.4 Solidification of droplets

Solidification in spray forming takes place in two distinct steps: typically half of the alloy latent heat is removed rapidly from the droplet spray created by gas atomization; the droplets are then constituted into a billet at deposition where the remaining liquid fraction solidifies relatively slowly. However, within the droplet spray, individual droplets have different thermal and solidification histories and depositing droplets may be solid, mushy, or liquid. Despite many studies of solidification behavior in spray forming, uncertainties and some misconceptions remain on how the solidification conditions in the spray and billet interact to give rise to the characteristic spray-formed microstructure comprising refined, polygonal/equiaxed primary grains with low levels of microsegregation. This article presents a simple numerical model for the spray-formed grain size arising from the deposition of the various droplets in the spray and combines insights provided by the model with previous investigations of the phenomena occurring during and immediately after deposition to propose a comprehensive description of the important solidification behavior during spray forming. Remelting, grain multiplication, thermal and elemental equilibration, and microstructural coarsening are proposed to play a critical role in the evolution of the spray-formed microstructure [48].

Models and experimental measurements show that small droplets (<50 μm) very rapidly become fully solid prior to deposition, 50-200 μm droplets will be typically semi-solid and droplets of diameters >200 μm will be liquid at deposition. The range of droplet dynamic and thermal histories results in a billet top surface of 0.3 to 0.6 solid fractions. Some solid droplets will bounce or splash-off the billet top surface or be directed out of the deposition region by turbulent gas movement in the chamber. The proportion of droplets that impact the surface compared to the proportion that are incorporated into the billet has been termed the 'sticking efficiency'. Droplets which impinge on the preform surface may be either fully liquid, mushy or fully solid, and the substrate surface itself may also be fully liquid, mushy or solid [49].

Fig. 2.16 shows schematically the changes in solid fraction during the spray forming process as a function of axial distance from the point of droplet atomization. The range of droplet solid fractions depositing at the billet surface equilibrate in the region of the billet top surface, labelled the equilibration zone, and the billet solid fraction (ignoring any radial variations across the billet) then gradually increases as the billet is slowly withdrawn to maintain a constant spray distance. Fig. 2.16 also indicates the smallest solid droplets seeded in the gas

flow, larger solid particles undergoing reheating and remelting, and mushy particles undergoing thermal shock and breakup (grain multiplication)[50].

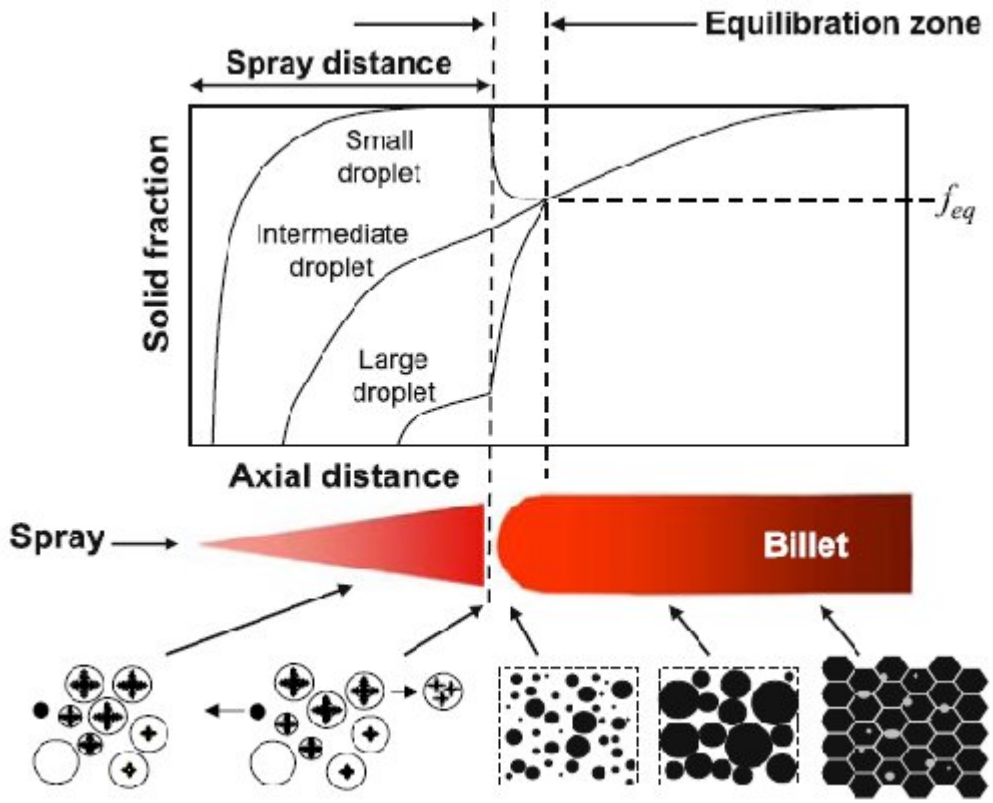

Fig2.16: Schematic representation of the changes in solid fraction during the spray forming process and the accompanying change in microstructure prior to and after droplet deposition.

Dendrite fragmentation takes place when droplets, in which dendritic solidification has occurred in flight, impact at high velocity onto the surface of the preform. The fine, pre-solidified particles or the dendrite fragments appear to re-melt in the liquid metal. The pre-solidified particles and coarse, fully molten particles add to the solid and liquid content at the surface of the preform. Thus, the preform surface consists of a mixture of dendrite fragments, pre-solidified particles and liquid metal [51].

Solidification probably arises from either the remains of the dendrite fragments, which provides a high density of nucleation sites in the liquid, or the solid particles in a non-dendritic mode. Rapid solidification occurs by convective cooling to the relatively cold atomising gas as it flows over the surface of the preform. The turbulence, which results from the mechanical momentum transferred by high velocity droplets to the deposition surface,

provides local homogeneity in terms of both temperature and composition. This results in an equiaxed morphology, which is typified by non-dendritic and spherical grains. Another possible mechanism for the origin of the equiaxed grain morphology is a solid state recrystallization reaction in the deposit during or after deposition. In this case, the thermal stresses generated during solidification provide the driving force for the reaction [40].

2.6.7.5 Mechanism of microstructure formation

The microstructure of spray-deposited materials is typically characterized by the absence of macrosegregation, and the presence of equiaxed grains with interdispersed, micrometer-sized pores. Macrosegregation is typically absent as a result of the fact that spray-deposited materials are formed by the gradual deposition of individual droplets, and consequently the segregation distance of alloying element is limited by droplet size. The grain morphology of spray-deposited materials is consistently reported in the literature to be equiaxed.

Despite numerous investigations, a quantitative understanding of the relevant thermal, momentum and solidification mechanisms that govern microstructure evolution during deposition has yet to be established. There are various mechanism that have been proposed to rationalize the formation of equiaxed grains during deposition. These may be generally grouped into two categories [52]:

a) Nucleation-limited Mechanisms

b) Growth-limited Mechanism

a) Nucleation-limited Mechanisms: The proposed nucleation-limited mechanisms for equiaxed grain formation are primarily qualitative. In early spray deposition studies it was argued that the formation of equiaxed grains could be rationalized on the basis of dendritic arm fragmentation and grain multiplication during deposition. Such processes occur in the liquid or semisolid interaction domain at the upper surface of spray-deposited performs as shown in Fig.2.17 dendrite arm fragmentation is also shown in this figure. The grain size in spray-deposited material should be less than the average spacing of the fragments. On the basis of this mechanism, the smallest grain size will be limited by the number of available nuclei in the semi-liquid layer.

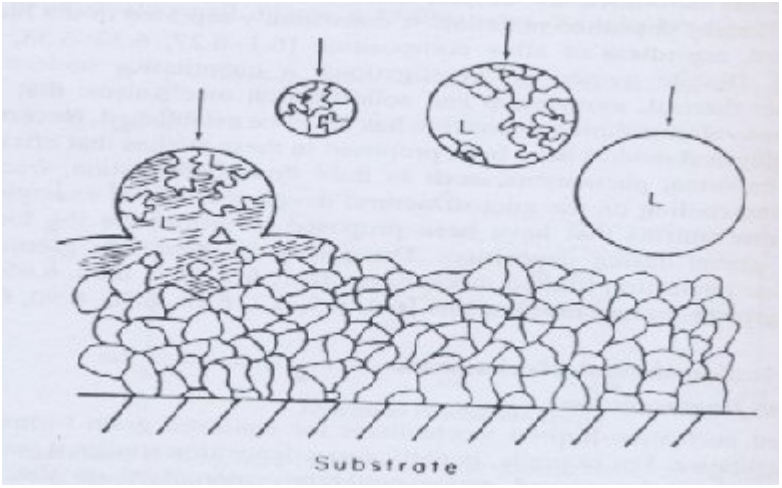

Fig2.17: Dendrite arm fragmentation during impingement and upper layer condition during spray deposition [52].

b) Growth-limited Mechanism: This mechanism has been proposed in an effort to quantitatively correlate grain size and thermal history during rapid solidification. Such mechanisms recognize the effects of grain growth and coarsening during solidification and during post-solidification cooling on the final grian size. Grian size may be considered to be the result of a competition between nucleation and grain growth kinetics [52].

2.6.7.6 Porosity

In the as-sprayed condition, deposits always include some porosity, usually in the range 1 to 10 %. There are three types of deposit porosity:

- Gas entrapment: entrapment of the atomising/carrier gas occurs during the atomisation or deposition stages.
- Shrinkage porosity: forms during the solidification due to the decrease in molar volume.
- Intersplat porosity: at the deposit top surface, the holes or interstices may not to be filled because of an insufficient liquid metal presence [40].

Gas entrapment is a frequently encountered type of porosity in sprays formed deposits. An unreactive or inert atomising gas, which is trapped during deposition, causes a large amount of porosity. This gas entrapment can be eliminated by using reactive gases, which react with the metal or alloy [53].

A lower level of porosity in spray forming nickel-base superalloys is produced using nitrogen gas because the nitrogen reacts with certain alloying elements in the superalloy to form nitrides. In contrast, when nitrogen is used for spray forming copper, more than 1 %

porosity is formed, because nitrogen is inert with respect to copper. When compared to PM processing, spray deposition process offers specific advantages in terms of residual oxygen and hydrogen levels which are considerably lower as a result of the very short interaction time between the liquid metal droplets and the surrounding atmosphere. Furthermore, if any oxide film is formed during the flight of the atomised droplet, it is likely that it will be disrupted and finely dispersed when impacting the semisolid preform surface. This probably accounts for the better ductility and fracture toughness of SD products as compared to their PM counterparts [40, 52].

2.6.7.7 Process variables

In the process of spray casting, there are number of independent and dependent variables which major influence the metallurgical and other integrity of a spray deposit. Some independent process parameters are [40]:

1) Gas Pressure(in range of 0.5-1.0 MPa)
2) Molten Metal Superheat(typical range 10-200'C)
3) Melt Flow Rate
4) Substrate Position, i.e. the distance between the gas nozzles and the substrate(300-350mm or more)
5) Substrate motion, Which includes substrate rotation speed , withdrawal rate and tilt angle.

These independent parameters can be directly controlled during the process and affect a number of dependent process parameters. There are number of pre-set parameters which cannot be changed during the operation i.e.

1) Type of atomizing gas(Nitrogen and Argon)
2) Diameter of melt delivery tube
3) The automiser design
4) Substrate material

On the other hand, if most of the droplets in the spray and/or on the surface of the deposit are liquid, the metallurgical properties of the spray casting will be similar to those of a conventional casting. Thus, the ideal amount of liquid must be between these extremes.

Therefore, the process parameters should be controlled to produce the optimum mixture of liquid and solid droplets [40, 54].

CHAPTER - 3

LITERATURE REVIEW

3.1 Microstructural study and mechanical properties

Yan et al [55] have studied an aluminium alloy metal matrix discontinuously reinforced with silicon carbide particulates, which was synthesized using the spray atomization and co-deposition technique. Microstructural characterization studies were performed to provide an understanding of the intrinsic effects of carbide particulate co-injection into the aluminium alloy metal matrix. The results reveal the ageing kinetics to be altered by the reinforcing ceramic particulates. Ambient temperature tensile tests revealed that the presence of particulate reinforcement in the aluminium alloy metal matrix degrades both strength and ductility.

Lavervia [56] has studied the synthesis of discontinuously reinforced Metal-matrix composites using spray atomization and co-injection. A variety of processing techniques have evolved over the last two decades to optimize the structure and properties of particulate reinforcedinetal-matrix composites(MMCs). Among these, spray processes offer a unique opportunity to combine the benefit associated with fine particulate technology with in situ processing, and in some cases, near-net shape manufacturing. Spray processing generally involves mixing reinforcements and matrix under highly non-equilibrium conditions, and as a result, these processes offer the opportunity to modify the properties of existing alloy systems, and develop novel alloy compositions. In principle, such an approach will inherently avoid the extreme thermal excursions, with concomitant macrosegregation, normally associated with casting processes. Furthermore, this approach also eliminates the need to handle fine reactive particulates, normally associated with powder metallurgical processes.

Chaudhury et al [57] have the synthesized aluminium based metal composites by a new spray forming technique. In their investigation, Al-2Mg-7TiO_2 composite was successfully spray atomized and co-deposited on a rotating substrate. The authers describe the processing methodology for the fabrication of Al-TiO_2 composites,which involves simultaneous introduction of aluminium melt and rutile particles through concentric tubes followed by inert gas atomization and deposition on a rotating copper substrate placed vertically below the attomiser at some predetermined height. Mechanical and physical properties of as-cast and

composite materials are discussed. For comparison, Al-2Mg-5TiO_2 composite was also prepared by stir cast method and characterized.

Ferrarini et al [58] have studied the microstructure and mechanical properties of spray deposited hypoeutectic Al-Si alloy. The microstructure and the tensile properties of an Al–8.9 wt.% Si–3.2 wt.% Cu–0.9 wt.% Fe–0.8% Zn alloy processed by spray forming was investigated. The alloy was gas atomized with argon and deposited onto a copper substrate. The microstructure was evaluated by optical microscopy (OM), scanning electron microscopy (SEM) and energy dispersive X-ray spectroscopy (EDS). Small faceted dispersoids observed surrounding equiaxial α-Al matrix were identified by SEM–EDS as silicon particles. Sand cast samples with the same composition showed a columnar dendritic α-Al matrix, Al–Si eutectic, polyhedric α-AlFeSi and needle-like β-AlFeSi intermetallics. In the spray formed material the formation of the Al–Si eutetic was suppressed, and the formation of the α-AlFeSi and β-AlFeSi intermetallics was strongly reduced. The fine and homogeneous microstructure showed an aluminium matrix with grain size ranging from 30 to 40 μm, and particle size of the silicon dispersoids having a mean size of 12 μm. Room temperature tensile tests of the spray formed alloy showed relative increasing of strength and elongation when compared with the values observed for the conventionally cast counterparts. These results can be ascribed to the refined microstructure and the scarce presence of intermetallics of the spray formed material.

3.2 Effect of Si content on wear property

Wang et al [59] have studied the effect of Si content on the dry sliding wear properties of spray deposited Al-Si alloy. In this investigation, Al–12Si, Al–20Si and Al–25Si (wt%) alloys were synthesized by spray atomization and deposition technique. The wear resistance of the alloys was studied using a pin-on-disc machine under four loads, namely 8.9, 17.8, 26.7 and 35.6 N. The microstructures, worn surfaces and the debris were analyzed in a scanning electron microscope. It has been found that the effect of Si content on dry sliding wear of spray-deposited Al–Si alloy was associated with applied loads. At lower load (8.9 N), with increasing Si content, the wear rate of the alloy was decreased. At higher load (35.6 N), spray-deposited Al–20Si alloy exhibited superior wear resistance to the Al–12Si and Al–25Si alloys.

Cui et al [60] To develop advanced aluminum alloys with high silicon content, hypereutectic aluminum silicon alloys AlSix (x = 18, 25, and 35 wt.%) in the form of cylindrical billet have

been spray formed under different thermal conditions. To help in spray forming parameter selection and interpretation of experimental results, phase diagram of the alloys and their thermochemical data such as liquid fractions and enthalpies in function of temperature have been calculated. The spray formed hypereutectic Al–Si alloys are typically composed of refined and uniformly distributed primary silicon and modified eutectic. Thermal conditions and silicon content of the deposited materials have significant influence on the metallurgical quality of the spray formed Al–Si alloys. Strong cooling condition is required for spray forming Al–Si alloys with high silicon content.

3.3 Wear property of Immiscible Alloy

Gouthama et al [61] have observed spray forming and wear characteristics of liquid immiscible alloys based on Al–Pb and Cu–Pb systems were gas atomized and spray deposited over a copper substrate. Microstructural examination of Cu–20Pb alloy indicated an equiaxed grain morphology of the primary phase with dispersion of Pb particles along the grain boundary and inter-granular regions. A wide size rage of atomised powder particles of this alloy showed cellular-dendritic morphology of the primary phase. The microstructure of spray formed Al–4Cu–20Pb alloy revealed a uniform distribution of ultrafine Pb particles in Al-matrix in contrast to a bimodal size distribution of Pb particles in atomised powder particles. Microstructural homogeneity was observed in both the atomized powders and spray formed alloys. The wear rate of Cu–20Pb alloy was observed to be higher than that of Al–4Cu–20Pb alloy at low load and sliding velocity. However, the former indicated a low wear rate in severe wear regime of high load and sliding velocity. The mode of solidification of liquid immiscible alloys during spray forming process is discussed and the wear behaviour of these alloys is analysed in light of their microstructural features.

Rudrakshi et al [62] have studied spray forming of Al–Si–Pb alloys and their wear characteristics. A modified spray forming process is described to synthesize liquid immiscible alloys based on Al–Si–Pb system. The atomization of the melt was carried out at a gas pressure of 1.0 MPa and the nozzle to substrate distance was varied from 0.35 to 0.55 m. The microstructure and wear characteristics of the spray-deposits were investigated. The results invariably exhibited an equiaxed grain morphology of the primary α-phase with variation in grain size from 10 to 25 μm in addition to a uniform dispersion of ultra-fine particles of lead and globular silicon particles in Al-matrix. The size of Si particles varied from 0.5 to 5 μm and that of Pb particles from 0.1 to 25 μm with variation in deposition distance. The microstructural variation was also observed in different regions of the deposit.

The atomized powder particles revealed two different types of microstructures, the one showing a cellular-dendritic morphology of the primary α-phase whereas the other exhibited fine spherical Al-particles dispersed in the matrix of Pb-rich phase. The wear rate and the coefficient of friction of Al–Si–Pb alloy were observed to be lower than that of Al–Si alloy at loads varying from 10 to 90 N at a sliding velocity of 1.0 ms^{-1}. The possible reasons for this behaviour are discussed in the light of microstructural features of the alloy and the nature of the worn out surfaces of the wear test specimens.

Srivastava et al [63] observed microstructural features induced by spray forming of a ternary Pb-Sn-Sb alloy containing Pb–12% Sn–12% Sb with small addition of copper and arsenic was spray deposited employing two different atomization gas pressure and nozzle to substrate distances. The temperature of the spray-deposit was measured during deposition at a distance of 2 and 10 mm above the substrate-deposit interface. Thermal profile data indicated small variation in temperature with time during deposition stage whereas during post deposition stage an exponential decrease in temperature was recorded. Second phase particle size along the thickness of the deposit varied from 4 to 8 μm compared to 70 to 80 μm size of these particles in the as cast alloy. Maximum porosity occurred in the section of the deposit near the contact surface of the substrate and also in its peripheral regions. X-ray diffraction analysis exhibited the formation of additional Cu_2Sb phase in the spray-deposit and CuSn and $Cu_{3\times3}Sb$ phases in atomized powders compared to that of the as cast alloy. The microstructural evolution during spray deposition of this alloy is discussed.

Guo et al [64] observed tribological behavior of Al/SiC/Ni-coated graphite (Gr–Ni) hybrid composites with various amounts of Gr–Ni addition synthesized by the semi-solid powder densification method was studied. The SiC and nickel-coated graphite (Gr–Ni) particles are distributed quite uniformly in an aluminum matrix. Wear debris become smaller, which causes smaller electric contact resistance, as the amount of Gr–Ni addition increases. Seizure occurs for monolithic aluminum alloy, but no seizure occurs for Al/SiC and Al/SiC/Gr–Ni composites. The friction coefficient and its fluctuations decrease as the percentage of Gr–Ni addition increases.. Due to the ‘‘composite effects’’, wear rates of both the composite and counterpart increase as the amount of Gr–Ni addition increases up to 5% Gr–Ni addition, then drop for 8% Gr–Ni addition. The wear rates of all the composites with Gr–Ni additions are higher than the wear rate of base Al/SiC material with no Gr–Ni addition. Therefore, the composites incorporating graphite do not work for wear reduction, as the debit in mechanical properties is larger than the very small benefit in friction reduction.

CHAPTER - 4

EXPERIMENTAL WORK

In the present work LM 13 alloy has been chosen for matrix alloy as it is used as commercial piston alloy and contains around 1% Mg which is necessary for wetting of dispersoid in the matrix. The reinforcement of SiC and additive immiscible element Sn is used for the study. The series selected for the work is as follow:

1. LM13 base alloy spray formed
2. LM13/SiC
3. LM13-5Sn/SiC
4. LM13-10Sn/SiC

4.1.1 Matrix material

Commercial grade near eutectic Al-Si alloy (LM13) was used in the present investigation. LM13 alloys was obtained in the form of ingots and cut it into small pieces by an electric power saw in order to feed the crucible properly. The compositional analysis of LM13 alloy is given in the Table 4.1

Table 4.1 Compositional analysis of LM13 alloy

Si	Fe	Cu	Mn	Mg	Zn	Ti	Ni	Pb	Sn	Al
11.800	0.365	1.230	0.411	0.940	0.210	0.0254	0.940	0.0289	0.005	Balance

4.1.2 Reinforcement material

Silicon carbide (SiC) particles were used as reinforcement material. Particle size of as received silicon carbide was in the range between 63-200 μm. The reinforcement particle were sieved and required particle size 106-125 μm were selected for the experimentation.

4.1.3 Process description

The spray deposition system basically consists of a spray assembly to produce spray of fine droplets and an atomization chamber wherein spray atomization takes place in an inert gas atmosphere. The alloy is melted in a graphite crucible placed in an resistance heating furnace. The molten metal is poured through the crucible into the atomization zone. The atomization zone consist of a convergent-divergent nozzle.

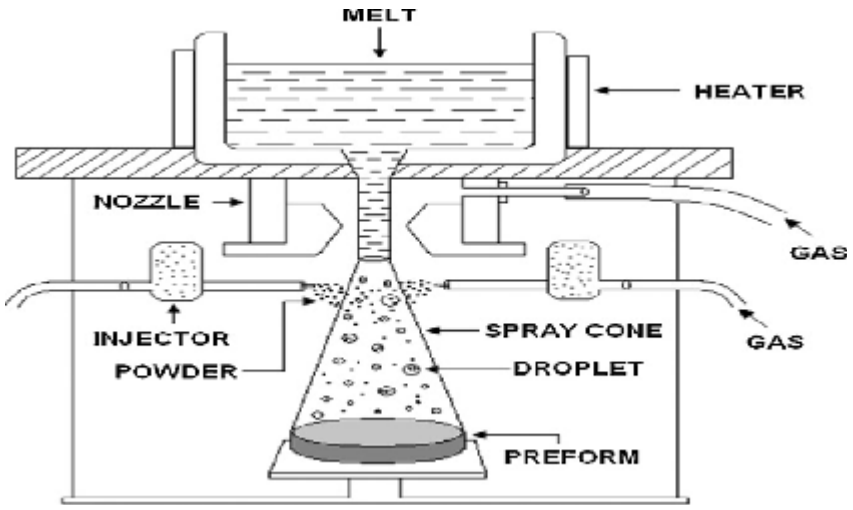

Fig.4.1. Schematic diagram of spray forming process.

In the atomization region, the molten metal stream is disintegrated into spray of droplets by gas jets. The droplets are cooled by the gas stream and accelerated towards a deposition substrate on which they impinge and consolidate to form a coherent deposit. Reinforcement particulates are supplied to the matrix material in the spray cone at some distance from the atomization zone. This result in co-deposition of particulates with the matrix metal to give rise to a coherent preform of composite material. The reinforcing particles are injected in the spray using injectors under the effect of high pressure inert gas. The particles interact with the liquid droplets in the spray and travel towards the substrate. These are dragged by the droplets or pull under gravity.

4.1.4 Experimental procedure

The indigenously designed and fabricated convergent–divergent atomizer is used for gas atomization and spray deposition. For spray deposition, 1.5 kg charge of LM13 alloy was melted at 800°C in a graphite crucible under nitrogen atmosphere in a resistance furnace. On

reaching the desired temperature, the alloy was poured into a preheated crucible attached above the atomizer assembly. Before pouring the molten alloy high pressure (0.7 MPa) nitrogen gas was passed through the atomizer.


(a)


(b)

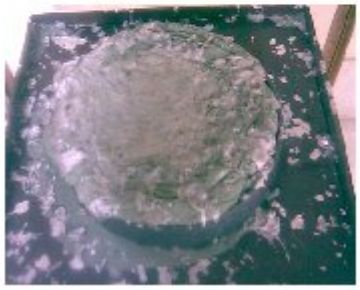
(c)

Fig.4.2.Spray forming process (a) set up of spray forming process, (b) spray forming nozzle and with 2 particle injectors,(c)spray formed perform above the copper subtrate

The melt flows through the melt delivery tube of inner diameter of 8mm concentrically fixed in the convergent–divergent atomizer. Simultaneously, preheated SiC particles (sieved in the particle range size 106–125μm) are fed into the spray cone with the help of two external powder injectors having orifice of 1mm placed around the melt atomizing section. The nozzle to substrate distance of convergent–divergent nozzle and substrate was kept at 300 mm. The atomized droplets get collected on the stationary copper substrate to make a solid preform of diameter 150 mm and thickness of 30 mm. From the preform, samples of dimensions 25mm×15mm×15mm were cut from different areas of the preform for further characterization. The over-spray powders were also collected for further examination.

4.1.5 Material characterization

The microstructural analysis has been done with the help of both optical (Eclipse MA-100, Nikon) and scanning electron microscope (JEOL,JSM-6510 LV, Japan) at various magnifications. the specimen were cut from different positions of the preform and prepared following the standard metallographic procedure of polishing and grinding. Over sprayed

powder particles were mounted with a cold setting acrylic resin to facilitate metallographic preparation. All the samples were etched in a Keller's reagent. The chemical composition of Keller's reagent is given in the table 4.5.

Table 4.2: Cheemical composition of Keller' reagent

Composition	Dist. Water	HNO_3	HCl	HF
Vol%	95ml	2.5ml	1.5ml	1ml

4.1.6 XRD

The as manufactured composite was characterized by X-ray diffractrometry to analyze the phase present in the material.

4.1.7 Hardness

The Rockwell hardness of the cast LM13 alloy, spray formed LM13 alloy and its composites reinforced with SiC particle has been measured at digital Rockwell hardness tester(model TRSND, fine manufacturing Industries India) machine using ball 1/16 inch ball indenter under 100kg load. Each reading is an average of at least five separate measurements taken at random places on the surface of specimens.

4.1.8 Wear testing

Wear test were conducted using polished pin samples with flat surfaces in the contact region but rounded in the corner and cleaned with acetone to remove dust or grease from the surfaces. Dry sliding wear tests were carried out against the counterface of a hardened and polished disk made of EN-31 steel having 65 HRC (Fig.4.3(b)) at a relative humidity of 36-56%. A pin-on-disc machine(Fig.4.3(a)) supplied by Ducom, Bangalore (model TR20-CH400) was used. The wear test pin samples have been prepared from the LM13 alloy and its spray form composites and the diameter of the pins are 8mm.

The test were conducted at the loads of 2.5, 3.5 and 4.5kg at the constant sliding velocity of 1.6m/s. However the wear characteristics has been noted down at two different temperature i.e. 50°C and 75°C.

(a)  (b) 

Fig.4.3. Wear testing machine (a) Wear and friction monitor, (b) pin and EN31-disk set up

The wear debris obtained after the 30 min of sliding of each test run were examined under SEM(JEOL, JSM-6510 VL,JAPAN). The worn surfaces of the samples were also examined under SEM to know the wear mode of the worn surfaces.

CHAPTER - 5

RESULTS AND DISCUSSION

5.1 X-ray diffraction analysis

The X-ray diffraction patterns of the prepared sample was recorded on Panalytical X'pert Pro MPD, Netherland using Cu K_α radiation (λ = 1.54 Å). The collected data were matched with reference data for identification of different phases. The XRD pattern (Fig.5.1) shows the presence of Al, Si, Sn and SiC in the composite. The peak intensity of Sn in LM13-10Sn/SiC(106) is greater as compared to the LM13-5Sn/SiC(106) due to higher amount of Sn addition in the composite. The reference sources for matching the peaks are Al (ICDD card no. 040787); Si (ICDD card no. 772111); Sn (ICDD card no. 040673) and SiC (ICDD card no. 742307).

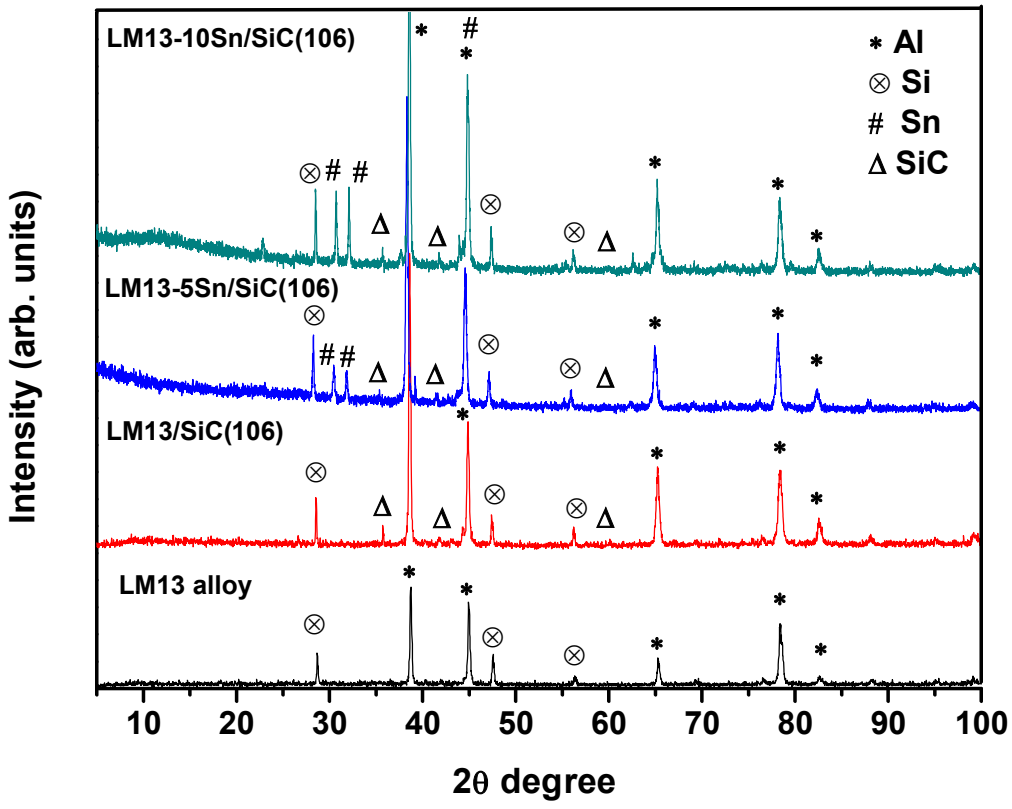

Fig 5.1: XRD pattern of LM13 alloy and spray formed composites.

5.2 Microstructural analysis

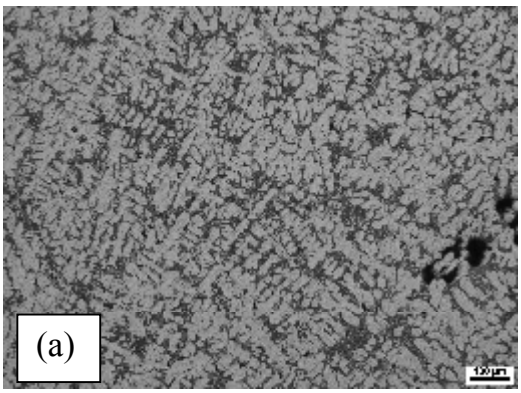

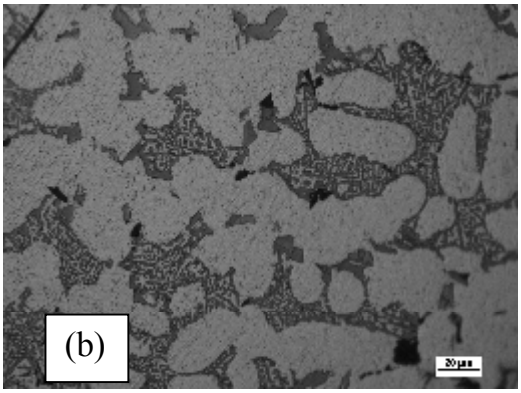

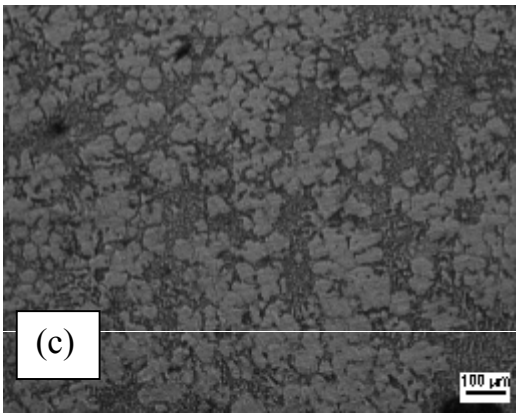

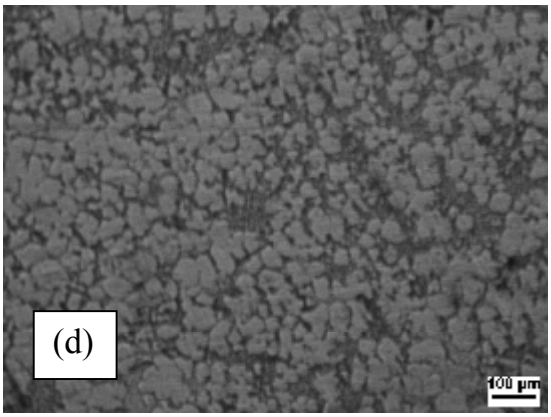

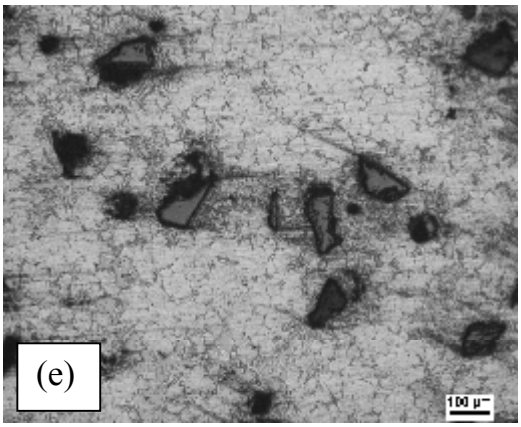

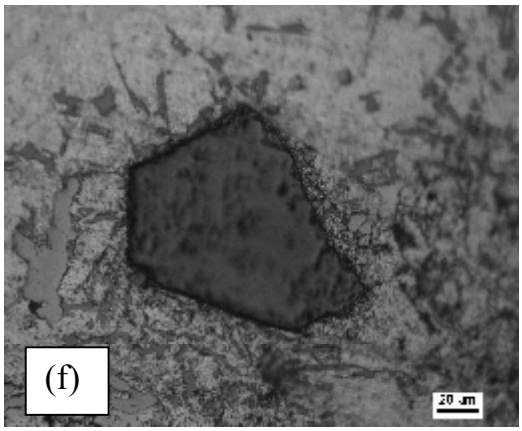

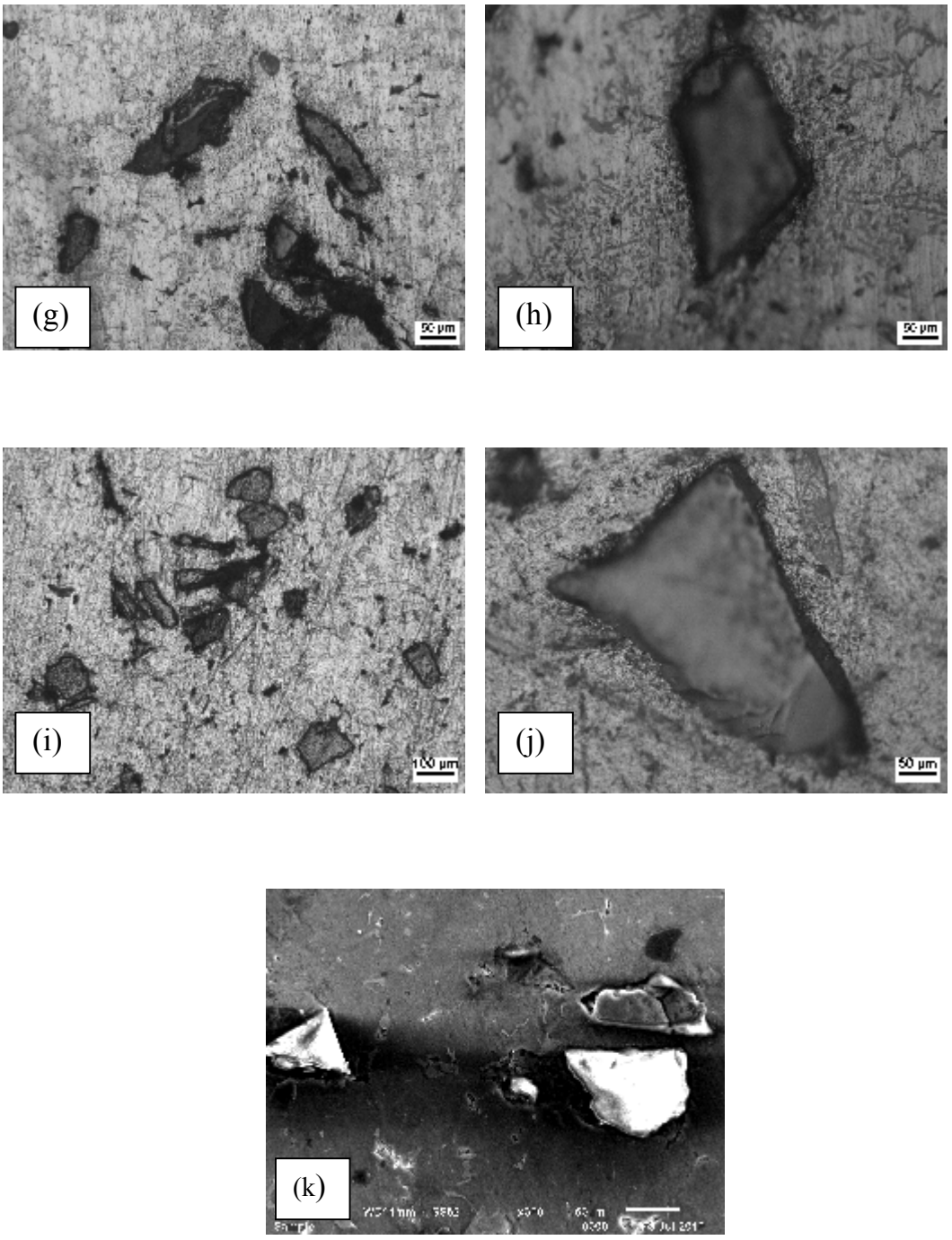

Fig.5.2. Micrographs of LM13 alloy **(a, b)** at 100X**,** and 500X, respectively; Spray Cast LM13 alloy (**c, d**) at 100X, and 500X respectively; Spray cast LM13/SiC(106) **(e, f)** at 100X and 500X respectively; Spray cast LM13-5Sn/SiC(106) **(g, h)** at 100X and 500X respectively; Spray cast LM13-10Sn/SiC(106) **(i, j)** at 100X and 500X respectively; SEM LM13/SiC(106) (**k**) at 300X.

The microstructures of the cast LM13 and its spray formed composites were examined under optical microscope are shown in Fig. 5.2. The cast LM13 alloy shows the dendritic morphology of α-Al (Fig. 5.2(a)) and eutectic Al-Si phase (Fig. 5.2(b)) in between the dendritic arms. The dendritic morphology of cast LM13 alloy structure has been eliminated in spray formed LM13 alloy. A different microstructure is observed in the spray deposit depending of the process parameters. After spray forming, LM13 alloy invariably indicate homogeneous microstructure with equiaxed α-Al grains (25-100μm) throughout the deposited material as shown in Fig.5.2 (c, d). Similar equiaxed morphology has been reported by other researchers [63]. The white phase as shown in all the microstructure is the Al-phase, it is the matrix phase. And dark phase which are equally distributed in the microstructure is the eutectic silicon phase. Eutectic Si phase is present in flowery pattern around the equiaxed Al-grains (Fig.5.2 (c, d)).

The microstructure analyzed at 100x of LM13/SiC, LM13-5Sn/SiC and LM13-10Sn/SiC composite processed by spray forming process is shown in Fig.5.2 (e, g and i) respectively. These micrographs show the equally distribution of SiC particle in matrix phase. The particle-droplet interaction in the spray and also on the deposition surface plays a crucial role in evolution of microstructure during spray deposition. As the SiC particle collide with the melt, due to difference in the temperature of SiC particle and molten matrix a thermal gradient has been generated which give rise the splat quenching in the region around its deposition as shown in Fig.5.2 (f, h and j) at 500X. The generation of small silicon globules around the SiC particle and short network of Si is also visible in the micrographs. Fig.5.2(k) shows the secondary electron SEM image of SiC particle in the matrix phase.

5.3 Over Spray Particle

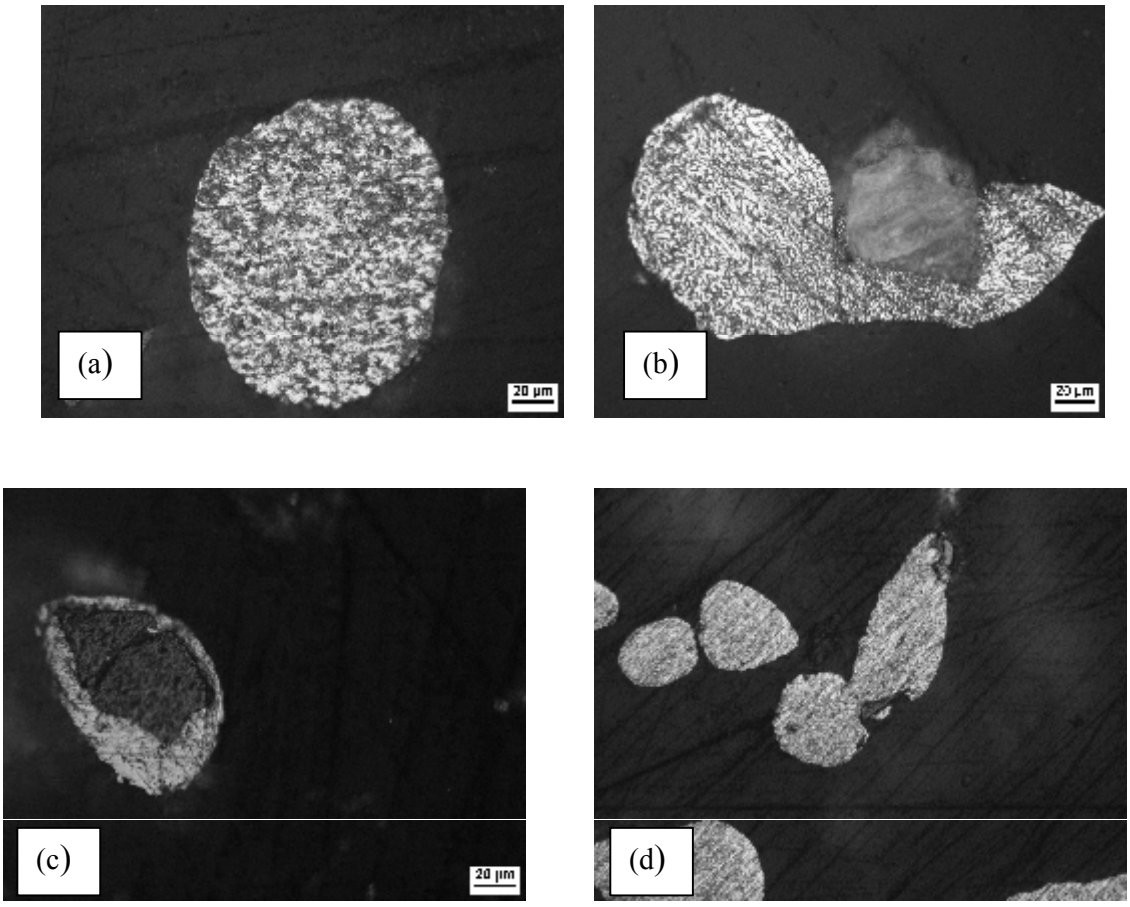

Fig.5.3 (a-d) Optical micrograph of over spray particle of LM13 alloy/ SiC composite

The overspray powder collected after experimentation has been mounted in the acrylic. The optical micrographs taken after grinding and polishing for the particles are shown in Fig. 5.3(a-d). The small dendrites and globular Si are clearly visible in overspray powder fig. 5.3(a). In spray forming process the second phase particles are incorporated into the matrix in various modes. These features are clearly observed in the microstructure of over spray particles as shown in Fig.5.3 (b-d). The collision of particulate and molten alloy is clearly visible in Fig. 5.3(b). The complete penetration of the reinforcement in the atomized droplet is shown in Fig. 5.3(c). The micrograph Fig. 5.3(d) shows the droplet-particle interaction during atomization giving rise to cellular-dendritic morphology.

5.4 Hardness

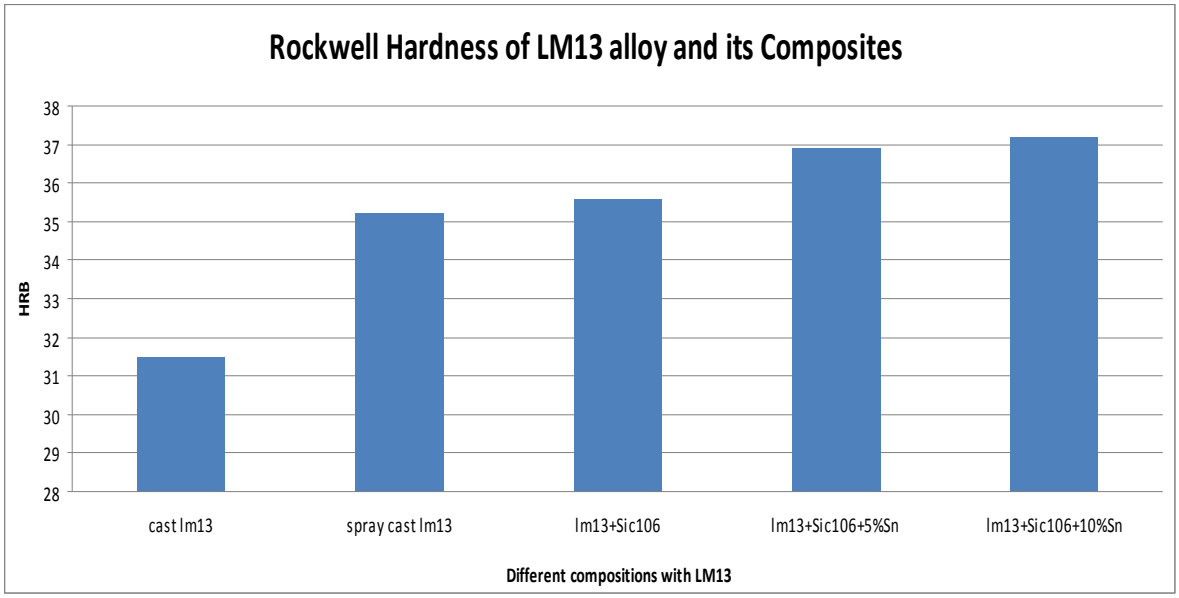

Fig. 5.4 Rockwell hardness of LM13 alloy and its composites.

The mechanical properties like hardness were evaluated at B-scale of Rockwell harness tester for cast LM13 alloy and its composites and are plotted in Fig.5.4. The hardness of cast LM13 base alloy has been found to be 31.46HRB. However, the hardness increases upto 35.2HRB on spray forming of LM13 alloy. This can be related to the refinement of microstructure by spray forming process as shown in Fig.5.4 (a-d). The embedment of SiC particle increases the hardness of the alloy upto 35.6HRB. The hardness of the composite depends upon the hardness of embedded particle and hardness of matrix phase. On addition of 5% and 10% Sn, the hardness further raised to 36.9HRB and 37.2HRB respectively. Sn is working as a modifier of microstructure as the globular Si around vicinity of the particles are greater in and LM13-5sn/SiC106 (Fig. 5.2 (h)) than LM13/SiC106 (Fig. 5.2 (f)). Sn is segregated along the grain boundary of Al-grains. Hence, spray formed structure, reinforcement of SiC particle and addition Sn modifier are increasing the hardness of material as compared to base alloy.

5.5 Wear characteristics

5.5.1 Effect of sliding distance

The wear rate behaviour against sliding distance has been found at each load for LM13 alloys and its composites reinforced with SiC dispersoids as shown in Fig.5.5(a,b)-5.9(a,b) at 50°C and 75°C. Fig.5.5(a) shows the results of wear rate for cast LM13 alloy at different loads and constant sliding velocity of 1.6ms^{-1} at 50°C. Under an applied load two different type of wear behaviour can be predicted from the curves. Fluctuating, unstable and greater wear at the initial stage corresponds to the run in wear. On the other hand constant wear rate has been obtained at later stage corresponding steady state wear. For both cast and spray formed LM13 alloy a steady state is approachable after 500m sliding distance for all applied loads except higher load of 4.5kg. Generally wear rate follows the increasing trend with ascending order of applied loads for all compositions. Similar findings have been obtained in the Al-2Mg-TiO_2 system for spray and stir cast composites [65].

In both cast and spray formed LM13 alloy mode of stabilization of wear gets delayed for 4.5 kg load. This might be due to the increase in frictional force exerted on the rubbing surfaces at higher load. It would lead large amount of energy to dissipate in the form of heat increasing temperature of the pin which causes the delay in steady state. The splitting of the peaks at this load in running- wear regime can be seen in Fig.5.5(a) and Fig. 5.6(a,b) corresponds to the debris build up phenomenon. The mechanical welding of the plastically deformed material at the edges of the pin leads to rise in fluctuating wear rate in the plots. On comparing the wear rate at each load it has been found that the wear resistance offered by spray processed composite is higher than base LM13 alloy and reinforced SiC composites as shown in Fig. 5.7-5.9 (a,b). This shows the good interfacial bonding of SiC particle and matrix phase. Moreover, wear rate stabilization for SiC reinforced LM13 composite (Fig. 5.7) is almost half the sliding distance (250m) as compare to cast or spray formed LM13 alloy. Moreover, wear rate in LM13-10Sn/SiC reinforced composite (Fig.5.9) is lower than LM13-5Sn/SiC reinforced composite (Fig.5.8). This might be due to the increase in the lubrication effect provided by Sn between the rubbing surfaces. Further, microstructural analysis of the wear surfaces and wear debris is necessary to understand completely the wear mechanism.

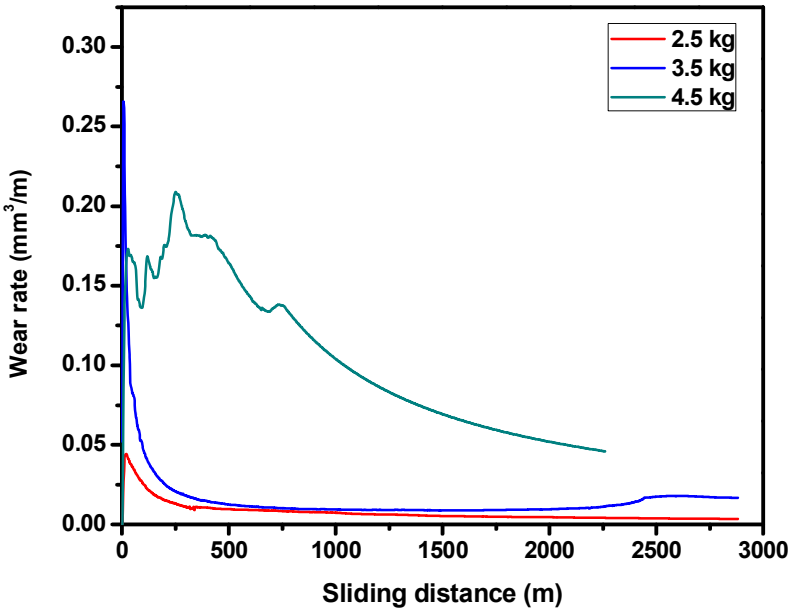

(a)

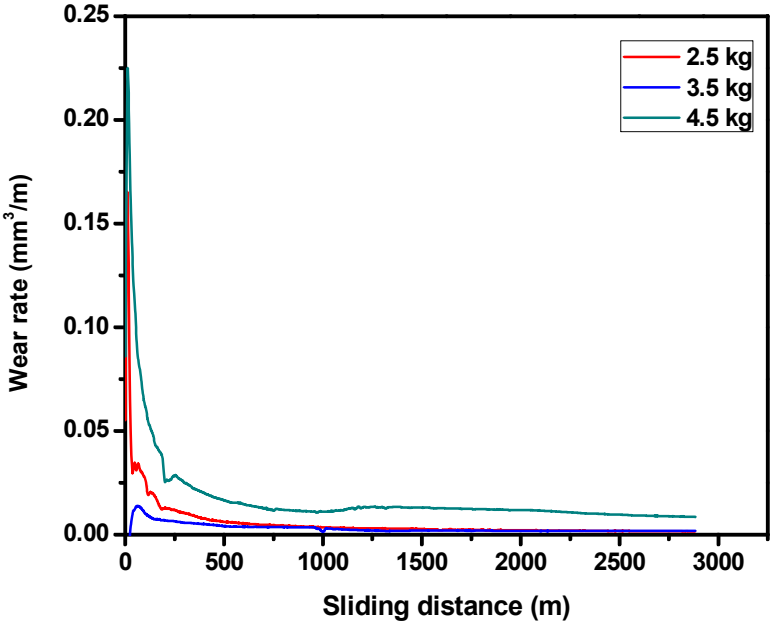

(b)

Fig.5.5: Variation of wear rate vs. sliding distance for cast LM13 alloy at (a) 50°C (b) 75°C.

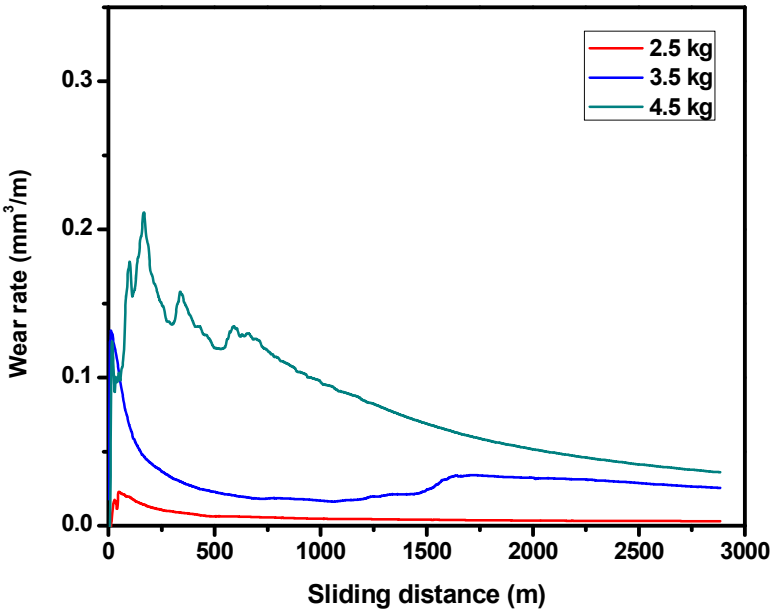

(a)

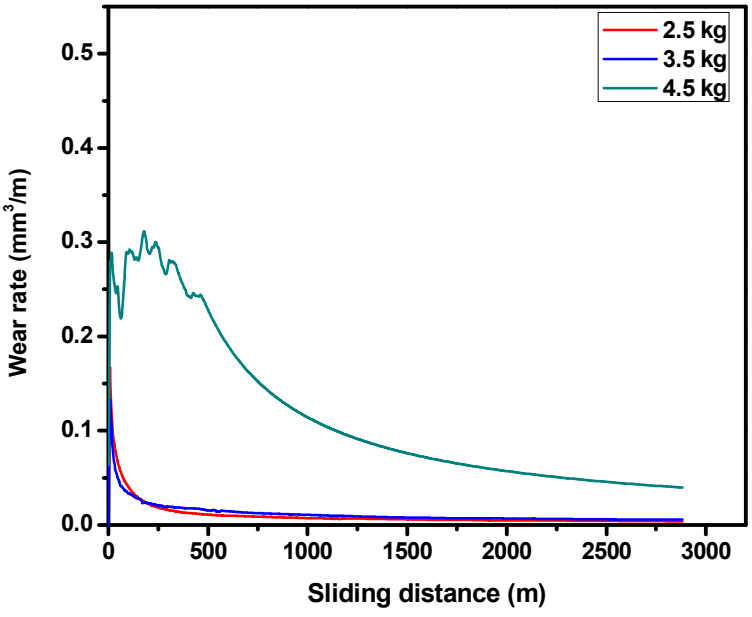

(b)

Fig5.6: Variation of wear rate vs. sliding distance for spray formed LM13 alloy at (a) 50°C (b) 75°C.

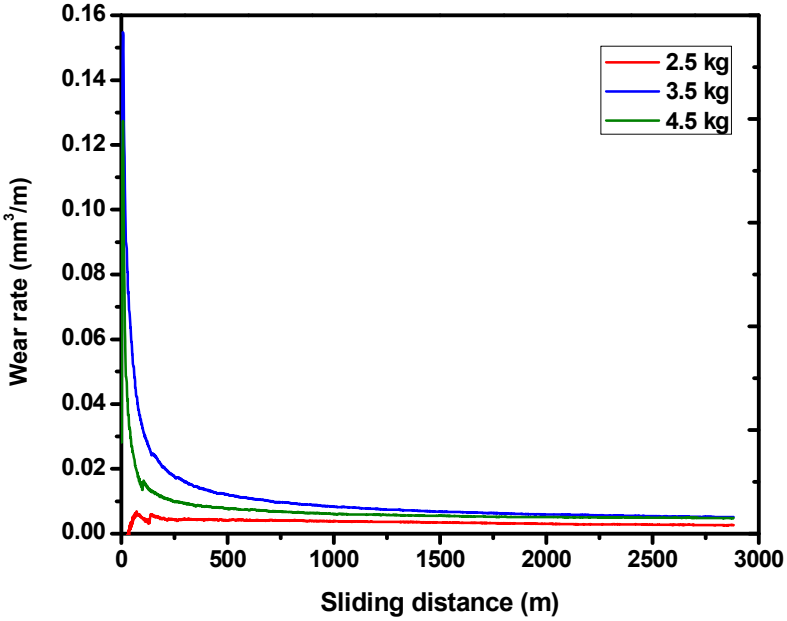

(a)

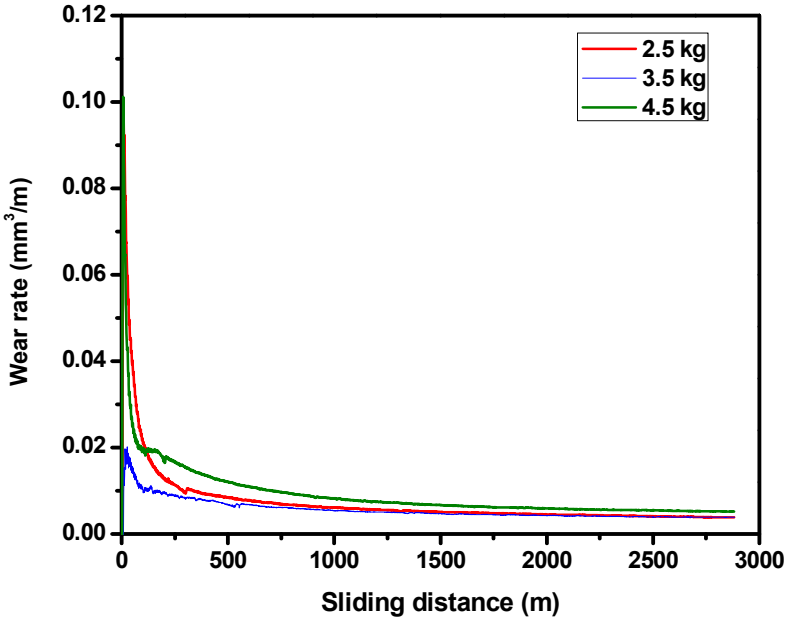

(b)

Fig.5.7: Variation of wear rate vs. sliding distance for spray formed SiC (106) reinforced LM13 alloy at (a) 50°C (b) 75°C.

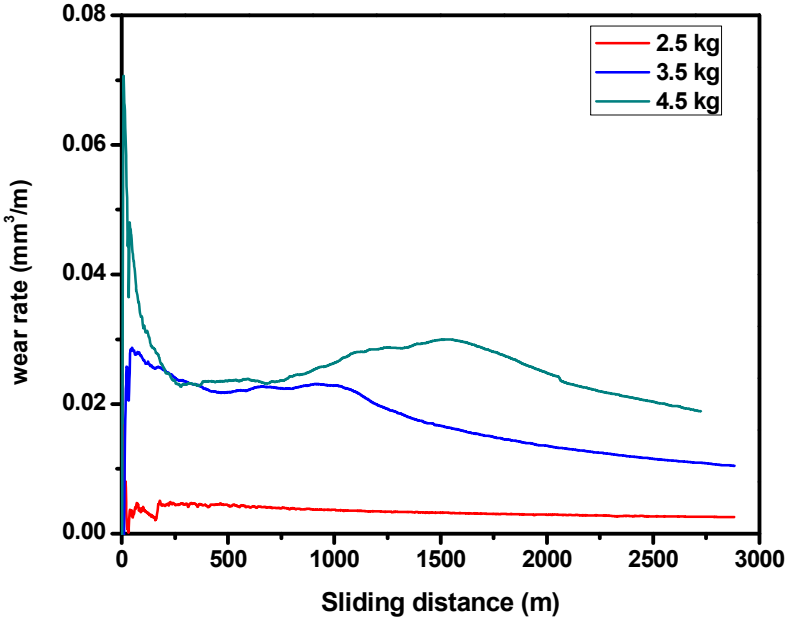

(a)

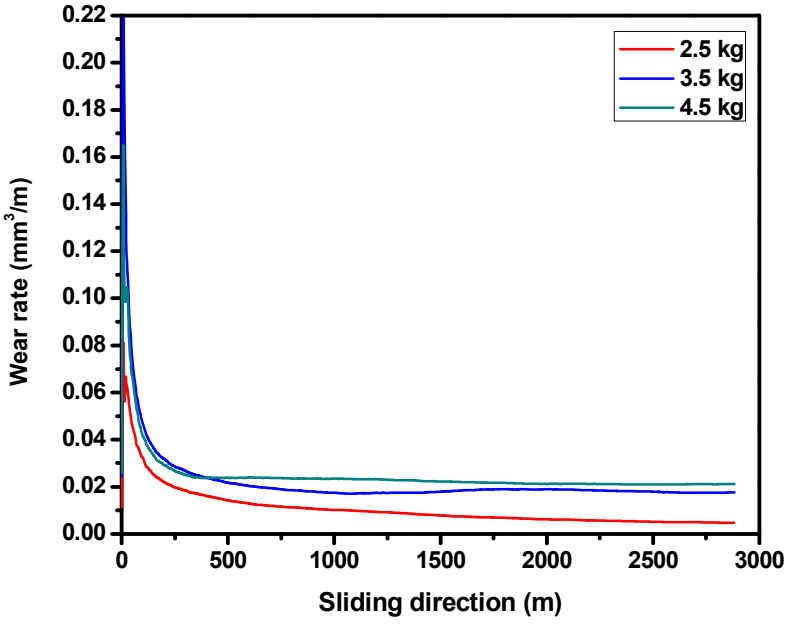

(b)

Fig.5.8: Variation of wear rate vs. sliding distance for spray formed SiC (106) reinforced LM13-5Sn alloy at (a) 50°C (b) 75°C.

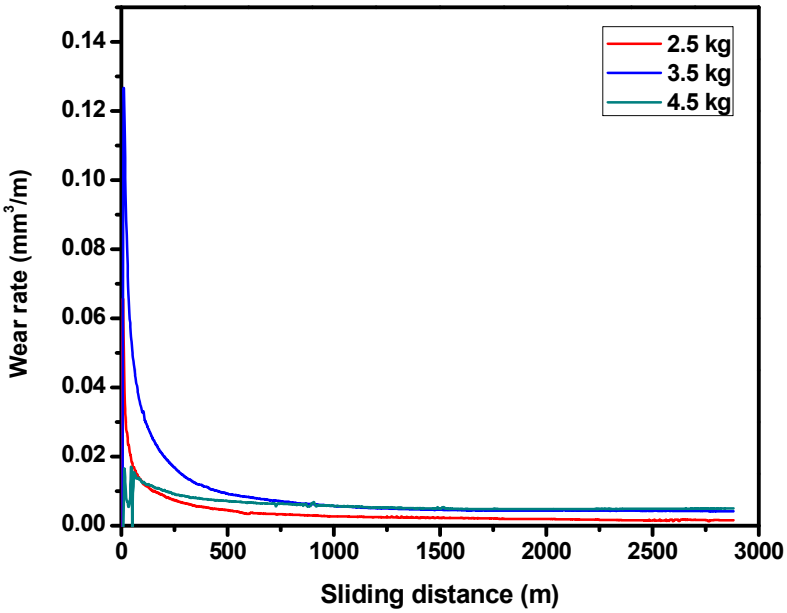

(a)

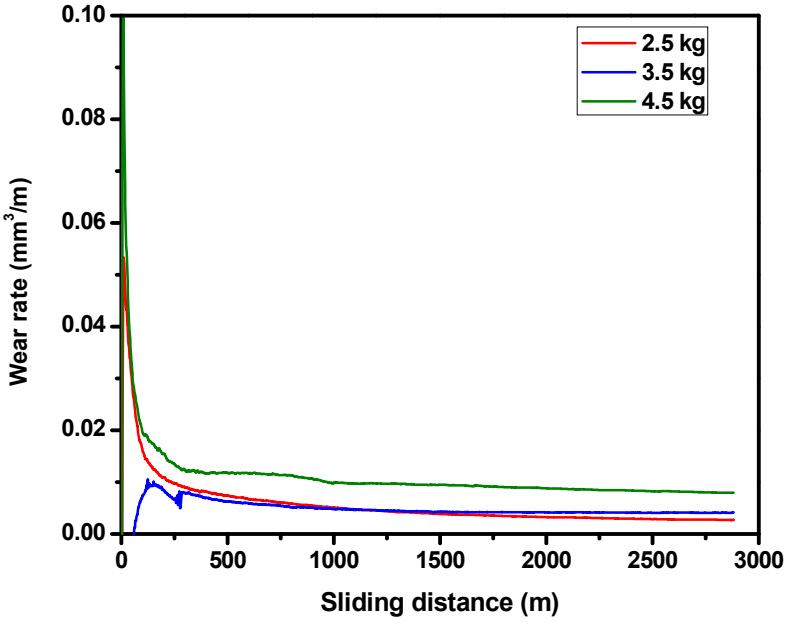

(b)

Fig.5.9: Variation of wear rate vs. sliding distance for spray formed SiC (106) reinforced LM13-10Sn alloy at (a) 50°C (b) 75°C.

5.5.2 Effect of composition and temperature

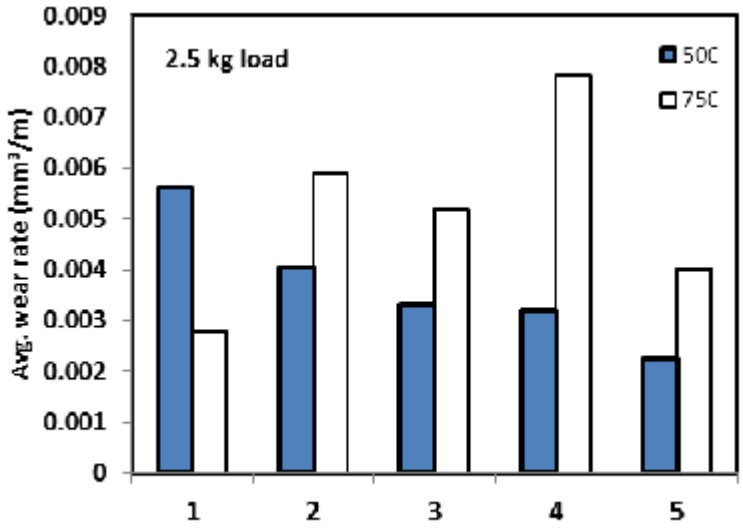

(a)

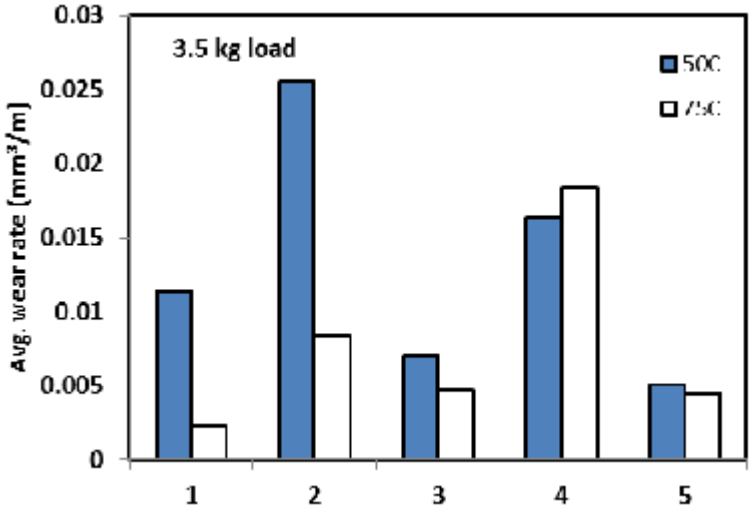

(b)

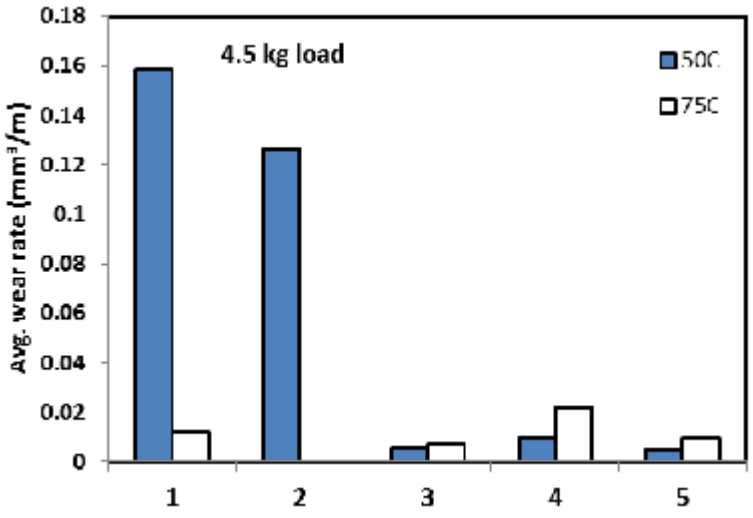

(c)

Fig.5.10: Average wear rate different compositions (**1**-cast LM13; **2**-spray formed LM13; **3**-LM13/SiC106; **4**- LM13-5Sn/SiC106; **5**- LM13-10Sn/SiC106) at 50°C and 75°C for (**a**)2.5 kg, (**b**)3.5kg and (**c**)4.5kg load.

The average wear rate has been calculated for each load after the steady state is approached i.e. after 500m sliding run. The results of average wear rate have been shown in the Fig. 2 where the averaged wear rate has been plotted against various compositions at both the temperatures 50°C and 75°C. At 50°C, it has been found that for 2.5kg and 4.5kg load spray formed composites are imposing greater resistance to the wear as compared to cast LM13 alloy. However, the data collected at 3.5 kg load is conflicting which might be due to the change in the mode of wear in both alloy and composite. At higher 75°C temperature and higher load also composite behaves well in resisting wear. But at lower load and higher temperature composites are less effecting in resisting wear. From all the five compositions LM13-10Sn/SiC106 has offered the good wear characteristics at lower and higher temperatures due to the higher content of Sn additive in the LM13 alloy which caters lubrication effect. All the summarized results of wear rate have been tabulated in the Table 1 given below.

Table 5.1: The average wear rate for various compositions and temperatures.

	Avg. wear rate (mm^3/m) for cast LM13		Avg. wear rate (mm^3/m) for spray formed LM13		Avg. wear rate (mm^3/m) for LM13/SiC_{106}		Avg. wear rate (mm^3/m) for LM13-5Sn/ SiC_{106}		Avg. wear rate (mm^3/m) for LM13-10Sn/ SiC_{106} (mm^3/m)	
	50°C	75°C	50°C	75°C	50°C	75°C	50°C	75°C	50°C	75°C
2.5	0.00562	0.00278	0.00405	0.0059	0.00332	0.00518	0.00319	0.00782	0.00225	0.00403
3.5	0.0114	0.00227	0.02555	0.00836	0.007	0.00472	0.01635	0.01839	0.00507	0.00448
4.5	0.1584	0.01166	0.12664	0.08393	0.00557	0.00693	0.00948	0.02216	0.00526	0.00937

5.4 Nature of Wear Surface and debris

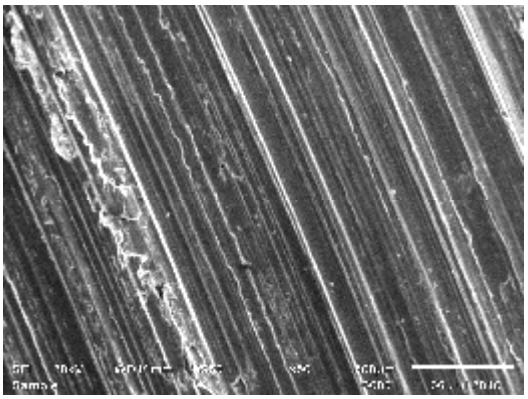

(a)

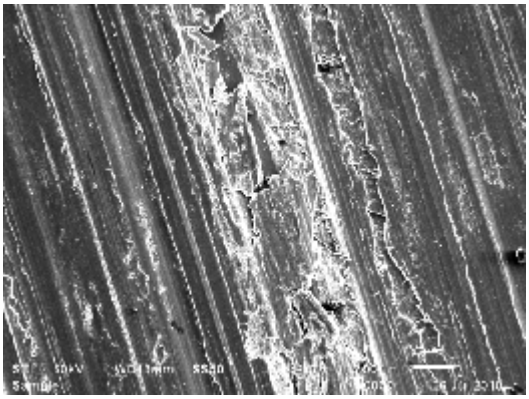

(b)

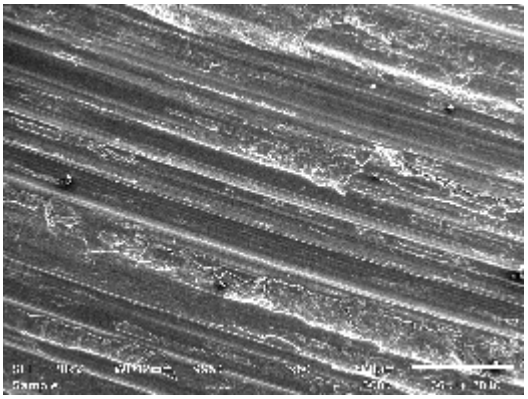

(c)

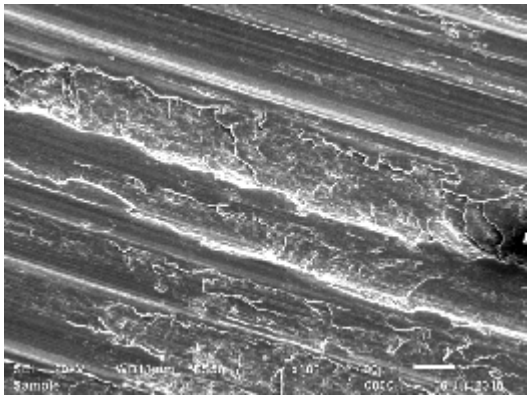

(d)

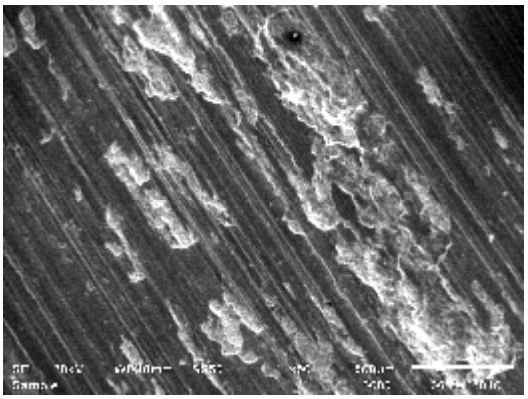

(e)

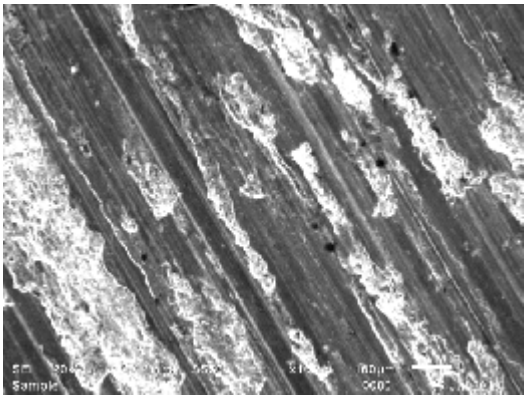

(f)

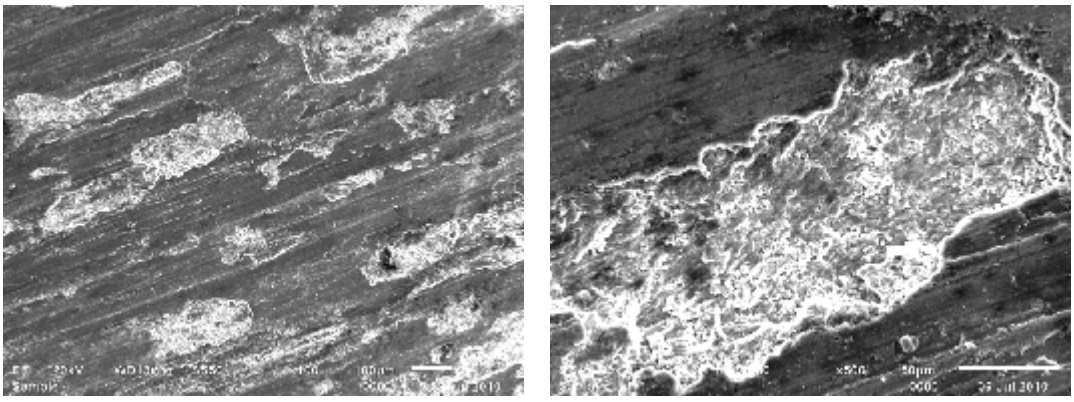

(g) **(h)**

Fig. 5.11 SEM micrograph of worn pin surfaces **(a-b)** LM13 alloy (75ºC) at 50x and 100x, respectively; (**c-d**) Spray cast LM13 alloy(75ºC) at 50x and 100x, respectively; (**e-f**) Spray cast LM13+SiC(106)+10%Sn (50^{o}C) at 50x and 100x, respectively; (**g-h**) Spray cast LM13+SiC(106)+10%Sn (75^{o}C) at 100x and 500x, respectively

The micrographs of the worn pin surface of base alloy and composites at 3.5kg load have been shown in Fig. 5.11 (a-h). One of the common features observed in all the micrographs is formation of grooves and ridge running parallel to the sliding direction in both base alloy and composite. These wear scars are the primarily characteristic of abrasive wear.

It has been found that grooves shows the repetitive ploughing marks in Fig. 5.11(c,d) in spray formed LM13 alloy as compared to cast LM13 alloy (Fig. 5.11(a,b)). At high magnification micrograph in Fig. 5.11(b) indicates debris formation from the ridge as the crack propagates perpendicular to sliding direction in cast LM13 alloy.

The morphological features of spray form LM13 alloy and SiC particle composite show complete different worn surfaces than cast LM13 alloy and spray form LM13 alloy (fig.5.11 (e-h). Large elongated dimples can be seen in the sliding direction on the surface of SiC embedded LM13 material. The enlarged view of the dimple is shown in Fig. 5.11(h) indicates the formation of non-uniform tribolayer on the worn surface. Little more coarsening in grooves are clearly shown at 75ºC as compared to 50ºC in spray cast composite (Fig. 5.11(e, g).

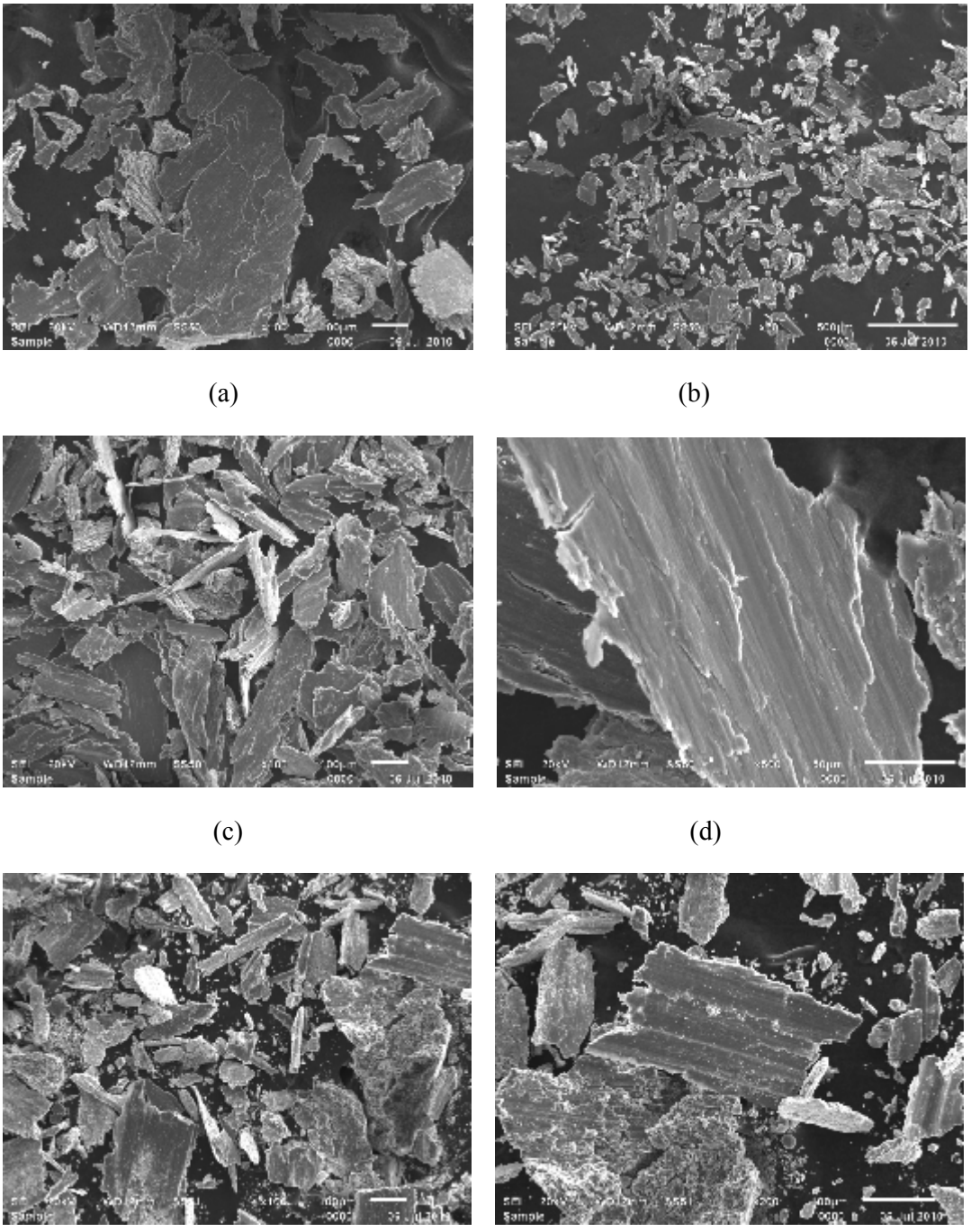

(a) (b)

(c) (d)

(e) (f)

Fig. 5.12 SEM micrograph of wear debris ,**(a-b)** LM13 alloy (75ºC) at 50x and 100x, respectively; (**c-d**) Spray Cast LM13 alloy(75ºC) at 100x and 500x, respectively; (**e-f**) Spray cast LM13+SiC(106)+10%Sn (75^{o}C) at 100x and 200x, repectively

The wear mechanism has been further correlated to the microstructural analysis of loose debris (Fig. 5.12) of LM13 alloy and spray formed composite at 75ºC and 3.5kg load.

On comparing Fig. 5.12 (a, c and e) at similar 100X magnification, it has been found that chunk of debris are found for LM13 alloy in Fig. 5.12 (a). It corresponds to the removal of material by delamination. Moreover, the morphology of debris reveals the metallic wear mechanism acting in the cast and spray formed LM13 alloy as shown in Fig. 5.12 (a,c). However, at similar load and temperature both metallic and oxide wear debris can be found in spray formed LM13-10Sn/SiC composite as revealed from Fig. 5.12 (e,f).

Since cast LM13 alloy sample is soft in nature as compared to spray formed composite, the metallic debris did not get oxidized so easily because higher thermal conductivity of the phases present in it. The metallic debris obtained in cast LM13 and spray cast LM13 as shown in Fig. 5.12(a-d). The fine cracks present on the surface of the debris also support the view that chunk of particle get removed from the surface during testing. The further reduction of the debris size is found due to the subsequent sliding of the flakes between the sliding surfaces as shown in Fig 5.12(b).

At higher magnification the wear tracks are clearly visible on the surface of the debris particles (Fig. 5.12 (d,f)). But in case of spray formed LM13-10Sn alloy/SiC composite oxide debris has also been obtained (Fig.5.12 (f)) along with metallic flakes. The morphological feature of debris indicates that metal is removed from surface which gets oxidized during ploughing in the course of sliding. The ploughing marks are clearly visible on the surface of metallic debris (Fig. 5.12 d and f).

CHAPTER - 6

CONCLUSION AND FUTURE SCOPE

6.1 Conclusion

The SiC particle reinforced LM13 alloy is successfully prepared with spray deposition technique. The hardness and wear characteristics of both LM13 alloy and composite s have led to the following conclusion:

1) The spray formed LM13 alloy exhibit equiaxed morphology of the primary Al-phase. The fine globular morphology of Si element is observed along the vicinity of SiC particulates in the matrix. As well as SiC particles are also equally distributed in the matrix material.

2) The hardness of spray formed LM13/SiC composite is higher than that of cast and spray formed LM13 alloy due to incorporation of ceramic particulates in the alloy. However, further increase in the hardness has been observed with increasing amount of Sn in the alloy.

3) All alloys showed increase in wear rate with applied load. However, at 50C both at higher and lower load spray cast LM13-Sn/SiC composite showed the highest wear resistance compared to that of cast LM13 alloy and spray formed LM13 alloy.

4) The scanning electron microscopy of worn surfaces and the debris particles of the alloys revealed that mode of wear in LM13 alloy is metallic wear mechanism as compare to the metallic-cum-oxidative wear mechanism in the LM13-Sn/SiC composite.

6.2 Future scope of study

One of the major advantages of spray forming is the ability to develop new alloys or products. Spray formed Al-Si alloy have been investigated and designed for space and automotive application because of reduced cost as compared to other manufacturing process. Spray formed Al-Si alloy have wide application because of attractive combinations of low coefficiant of thermal expansion, good wear resistance , good thermal stability.

However, further study is required for different reinforce particle size and alloying elements in different percentage for improving the structural and mechanical property as compared to present study.

For these purpose requirements and fundamental studies, many spray-forming R&D plants has been established notably at U.S. Navy Labs, Pennsylvania State University, Applied Research Labs, Advanced Institute of Science and Technology (Korea), National Cheng Kung University (Taiwan), IPEN (Brazil), Oxford University Centre for Advanced Materials and Composites (United Kingdom), Inner Mongolia Metals Institute (China), Bremen University (Germany), and the University of California at Irvine. However, in developing country like India this technique is still under progress for its commercialization. Therefore, a lot of future prospectus is related to this novel technique to develop new alloys and composites.

REFERENCES

1) S.K.Jagadeesh, "Journal of Materials Processing Technology", **210**,(2010), 618-623.
2) R.Schaller, "Alloys Compound" ,**355**(2003) 131.
3) Serdar Z.Elgun, "info.lu.farmingdale.edu/particlerc.JPG"
4) http://www.aviation-history.com/theory/composite.htm
5) Sanjeev Das, S. Das, K. Das, "Composites Science and Technology",**67**(2007) 746-751.
6) M.K. Surappa, "Journal of material processing Technique" ,**63**(1997) 325.
7) www.epfl.ch/people/cayron/Fichiers/thesebook-chap2.pdf.
8) O.Beffort, L.Rohr, W. Muster and K. Schlaepfer "Nachhaltige Material and Systemtechnik"(2000)21–28.
9) http://www.substech.com/dokuwiki/doku.php?id=metal_matrix_composites _introduction.
10) www.bcaa.com/images/content/BMW-engine-web.jpg.
11) www.troybuiltmodels.com/.../spareparts/acc6.jpg.
12) www.flexibleduct.com/.../thumbnail_3.jpg.
13) http://web.tradekorea.com/upload_file/prod/emp/2008/oimg_GC00184458_C.
14) William D.Callister, "Material Science and Engineering an Introduction", "Wiley and sons publication",**7th edition**,(2007)
15) M.K Surappa, Sadhana, "Aluminium Matrix Composites Challenges and opportunities" **Parts 1&2**, **28**(2003)319-334**.**
16) S.Bose,"Engineering properties of selected ceramic materials","The American Ceramic Society" (1966).
17) A. Banerji,M.K.Surappa and P.K. Rohatgi, "Metall. Trans. B",**14B** (1983)273.
18) S.C. Sharma, B.M. Girish, D.R. Somashekar, Rathnakar Kamath, B.M. Satish, "Composites Science and Technology", **59**(1999) 180.
19) Sanjeev Das, Siddhartha Das, Karabi Das,"Composites Science and Technology" **67**(2007) 746-751**.**

20) Fm Hosking, F.Folgar Portillo , R.Wonderlin ,R.Mehrabian,"Composite of aluminium alloys: fabrication and wear behaviour","Journal Material Science"**17**(1982)477-98.

21) S.M.L. Nai, M. Gupta, C.Y.H. Lim,"Composites Science and Technology" **63** (2003) 1895-1909.

22) T.W.Clyne,"Comprehensive Composite Materials","Metal Matrix Composites", **3**(2000)1-26.

23) R.Asthana,"Evolution of the interface","J. Mater. Sci."**33**(1998)1959-1980**.**

24**)** Cevdet Kaynak, Suha Boylu,"Materials and Design" **27**(2006)776-782.

25) N.Eustathopoulos, A.Mortensen, "Capillary Phenomena Interfacial Bonding and Reactivity","Fundamentals of Metal Matrix Composites"(1993)42-58.

26) D. J.Lloyd,I.Jin,"Comprehensive Composite Materials","Metal Matrix Composites"**3**(2000)1-21.

27) J.C.Lee,J.P.Ahn,Z.Shi,J.H.Shim,H.I.Lee,"Methodology to design the interfaces in SiC/Al composites","Metall. Mater Trans." **32A**(2001)1541-1550.

28) N.P.Suh,"The delamination theory of wear","Wear"**259**(1973)111-124.

29) www.wikipedia.com

30) T.W.Clyne,P.J.Withers**,** "An introduction to metal matrix composites Cambridge solid state Science series"(1993)509.

31) Mel M. Schwrtz,"Fabrications of Composite Materials", "American Society for Metals",(1985).

32) J.M. Torralba, C.E. da Costa, F. Velasco," Journal of Materials Processing Technology"**133**(2003) 203–206.

33) S.J. Harris,"New Light Alloys",(1990)4-21.

34) G.Greetham ,"Materials information Service AZoM",(2001)

35) Dr. Dmitri Kopeliovich,"substances & technologies", www.substech.com

36) Jasmi Hashim,"Jurnal Teknologi", **35**(2001)9–20

37) Udo Fritsching,“Spray simulation”,“Cambridge university press”, Chep.2,(2004)

38) Yunfeng Yang,“Method for spray forming a metal component and a spray formed metal component”(2009)

39) G.B.Rudrakshi,V.C.Srivastava, J.P.Pathak,“Spray Forming of Al-Si-Pb Alloys and their Wear Characteristics”,“Mat. Sci. & Engg.”,**383**(2004)30-38.

40) Elmas Salamci,“G U General of Science”,**17**(2004)155-173.

41) E.J.Lavernia and N.J.Grant,“Spray Deposition of Metals: A Review”,“Materials Science and Engineering”,**98**(1988)381-394.

42) S.N.Ojha,“Spray Forming: Science and Technology”, “Bull. of Materials Science”,**15**(1992)527-542.

43) B.A.Rickinson,F.A.Kirk,D.R.G.Davies,“CSD:A Novel Process for Particle Metallurgy Products”,“Powder Metallurgy”,**1**(1981)1-6.

44) X.Duan,Y.Hao,M.Yoshida,T.Ando,N.J.Grant,“Liquid Dynamic Compaction of Aluminium Alloy 7150”,“The International Journal of Powder Metallurgy”,**29**(1993) 149-160.

45) http://www.elliottequipment.com

46) Spray forming- Wikipedia, the free encyclopedia

http://en.wikipedia.org/wiki/Spray_forming.

47) S.N.Ojha,“Spray Forming: Science and Technology”, “Bull. of Materials Science”,**15**(1992)527-542.

48) P.S. Grant,“Metallurgical and Materials Transactions” **38**(2007)1520-1529.

49) P. S.Grant, “Spray Forming Progress in material science”,**39**(1995)497-545.

50) P.S. Grant,“The Minerals”,“Metals & Materials Society and ASM International” **38A**(2007).

51) E.J.Lavernia,J.D.Ayers,T.S.Srivatsan,“Rapid Solidification Processing with Specific Application to Aluminium Alloys”, “Int. Mater. Rev.”, **37**(1992)1-44.

52) Lavernia,Enrique J.,and Yue Wu,"Spray Atomization and Deposition",(1996)

53) P.Mathur, D.Apelian,A.Lawley,"Fundamentals of Spray Deposition via Osprey Processing","Powder Metalllurgy",**34**(1991)109-111.

54) A.Lawley,P.Mathur,D.Apelian,A.Meystel,"Spray Forming: Process Fundamentals and Control", "Powder Metallurgy",**33**(1990)109-111.

55) S. P.Yan, "An aluminum alloy metal matrix discontinuously reinforced with silicon carbide particulates"(1995).

56) E.J.Lavernia ,"Synthesis of Discontinuously Reinforced Metal-matrix Composites Using Spray Atomisation and Co-injection","J. Defence Science"**43**,(1993)301-321.

57) S.K.Chaudhury, S.C.Sivaramkrishnanand "A new spray forming technique for the preparation of aluminium rutile (TiO_2) in situ particle composite","J. of Materials processing Technology"**145**(2004).

58) C.F.Ferrarini, "Microstructure and mechanical properties of spray deposited hypoeutectic Al–Si alloy","Materials Science and Engineering" (2004)577–580.

59) F.Wang,H.Hu,Y.Ma,Y.Jin,"Effect of Si content on the dry sliding wear properties of spray-deposited Al–Si alloy",**25**(2003)163-166.

60) Z.D.Cui, S.L.Zhu,H.C.Man and X.J.Yang","Surface and Coatings Technology" 190(2005)309-313.

61) R.K.Gautam,S.Ray,S.C Jain,S.C.Sharma,"Wear" **265** (2008)902.

62) G.B. Rudrakshi, V.C. Srivastava, J.P. Pathak and S.N. Ojha,"Spray forming of Al Si–Pb alloys and their wear characteristics","Mater. Sci. Eng.", **383** (2004)30–38.

63) V. C. Srivastava,Anish Upadhyaya and S. N. Ojha,"Bulletin of Materials Science",**23**(2000)73-78.

64) M.L.T. Guo and C.Y.A. Tsao,"Tribological Behavior of Aluminium/SiC/Nickel Coated Graphite Hybrid Composites","Mater. Sci. Eng",**333**(2002)134–145.

65) S.K. Chaudhary, A.K. Singh, C.S. Sivaramakrishnan, S.C. Panigrahi,"Wear and friction behavior of spray formed and stir cast Al–2Mg–11TiO_2 composites", "Wear",**258**(2005)759–767.